Journal of Astronomical History and Heritage, 18(1), 65–97 (2015).

AN HISTORICAL PERSPECTIVE ON THE SUSPECTED METEORITE IMPACT SITES OF TENNESSEE. 2: THE HOWELL STRUCTURE

J.R.H. Ford
Faculty of Sciences, University of Southern Queensland, West Street, Toowoomba 4350, Australia, and National Astronomical Research Institute of Thailand, 191 Huay Kaew Road, Suthep District, Muang, Chiang Mai 50200, Thailand, and Department of Physics and Astronomy, Middle Tennessee State University, Murfreesboro, Tennessee 37132, USA.
Email: jford@mtsu.edu

Wayne Orchiston
National Astronomical Research Institute of Thailand, 191 Huay Kaew Road, Suthep District, Muang, Chiang Mai 50200, Thailand.
E-mail: Wayne.Orchiston@narit.or.th

and

Ron Clendening
Tennessee Division of Geology, 13th Floor, L & C Tower, 401 Church Street, Nashville, Tennessee 37243, USA, and Faculty of Sciences, University of Southern Queensland, West Street, Toowoomba 4350, Australia.
Email: ron.clendening@tn.gov

Abstract: The Howell Structure is a suspected meteorite impact site in Tennessee, USA, and came to the attention of geologists during the 1930s. It was first investigated by Born and Wilson in 1937, and the few subsequent investigations that have occurred at this extensively eroded site have revealed the presence of breccias and the possible existence of shatter cones. However, cores drilled in the 1960s have recently been analyzed, and these provide evidence of shock metamorphism, suggesting that the Howell Structure is the eroded scar of a meteorite impact.

Keywords: Howell Structure, Tennessee, meteorite impact site,

1 INTRODUCTION

The State of Tennessee, located in the south-eastern United States, contains two confirmed meteorite impact sites, Wells Creek and Flynn Creek, and two suspected impact sites, Dycus and Howell (e.g. see Berwind, 2006, 2007; Deane et al., 2004; 2006; Evenick et al., 2004; Evenick, 2006; Ford et al., 2012; 2013; 2014; Milam et al., 2006; Mitchum, 1951; Price, 1991; Roddy, 1977a; 1977b; Schedl et al., 2010; Schieber and Over, 2005; Stearns et al., 1968; Wilson, 1953; Wilson and Stearns, 1966; 1968; and Woodruff, 1968). However, recently-published evidence derived from cores drilled at the Howell Structure in the 1960s suggests that this, too, may be meteorite impact scar. This site and the other three confirmed or suspected Tennessee impact sites are shown in Figure 1.

Three of these sites are found on the Highland Rim escarpment which surrounds the Nashville Central Basin in middle Tennessee, while the fourth site, the Howell Structure, is located on one of the numerous isolated Highland Rim residual areas that lie within the Central Basin, near its south-eastern boundary. Meteorite impacts most certainly also occurred elsewhere in the state, but as Woodruff (1968) has observed, the structural features of such sites would have been obliterated to the east of the Highland Rim, in the deformed rocks of the Appalachians, while impact craters in the western part of the state would have been covered by coastal plain marine and transitional sediments during the Mississippian Embayment (Miller, 1974). In this paper we present an historical review of investigations that have been carried out at the Howell Structure.

The Howell Structure is an "…intensely deformed area …" located in the Highland Rim of south-central Tennessee (Born and Wilson, 1939: 371). It

> … is a roughly circular feature about 2.5 km in diameter, comprising brecciated, deformed, and disturbed sedimentary strata … centered on the unincorporated village of Howell … (Deane et al., 2004: 1).

The regional dip in this area "… is to the south and is at an average angle of considerably less than 1° …" (Born and Wilson, 1939: 375).

Large creeks, such as Cane and Norris, have eroded valleys in this section of the Highland Rim to almost the level of the Nashville Central Basin (Born and Wilson, 1939). Although "No large creeks flow across the structure proper … Cane Creek borders the western and southern limits, and Buchanan Creek borders the easternmost areas. The tributaries of Cane Creek dissect a large percent of the deformed area …"

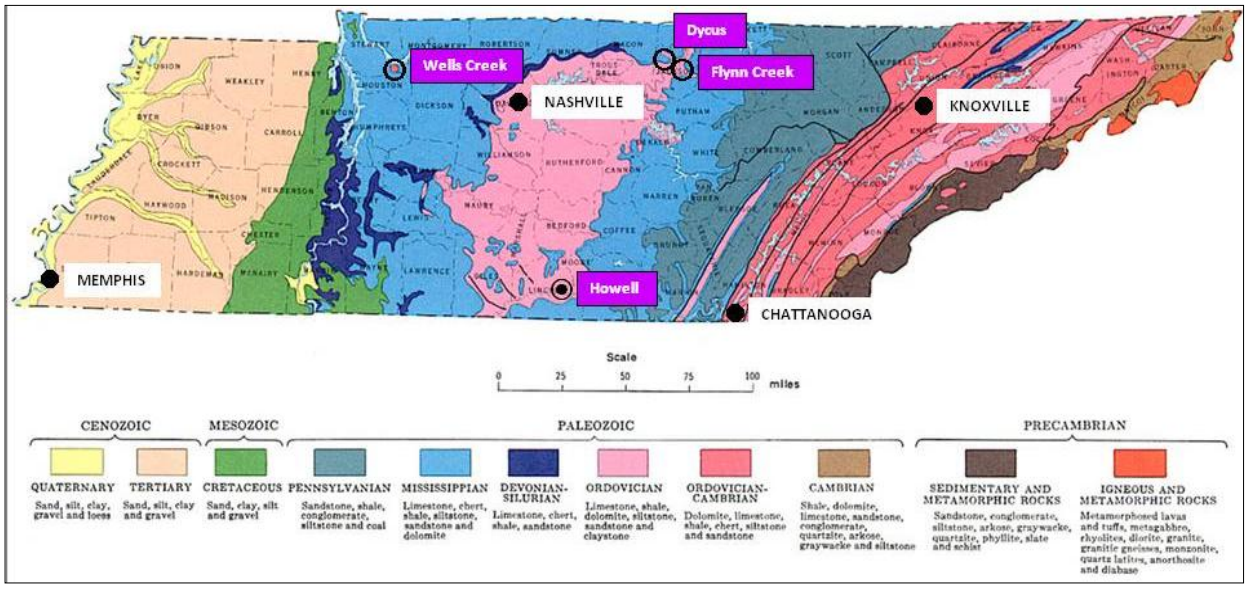

Figure 1: Generalized geological map of Tennessee showing the locations of the four largest cities (black dots) and the three confirmed meteorite impact sites (Flynn Creek, Wells Creek and Howell), and the Dycus suspected meteorite impact site. The Howell Structure, the subject of this paper, is located on a Highland Rim outlier remnant. The Highland Rim is the sky blue region on the map (base map after Tennessee Department Conservation, Division of Geology, 1966).

(Woodruff, 1968: 4). Narrow ridges between the creeks and streams are remnants of the Highland Rim with an average elevation of some 100 meters above the eroded valleys and Howell, for the most part, is some 16 meters above these valley floors (Born and Wilson, 1939; Woodruff, 1968). Deane et al. (2004: 1) note that

> The western two-thirds of the Howell Structure occur [*sic*] in rolling, grass-covered pasturland, while the eastern one-third consists of forested hills rising 130 m above the surrounding terrain. Exposures are limited …

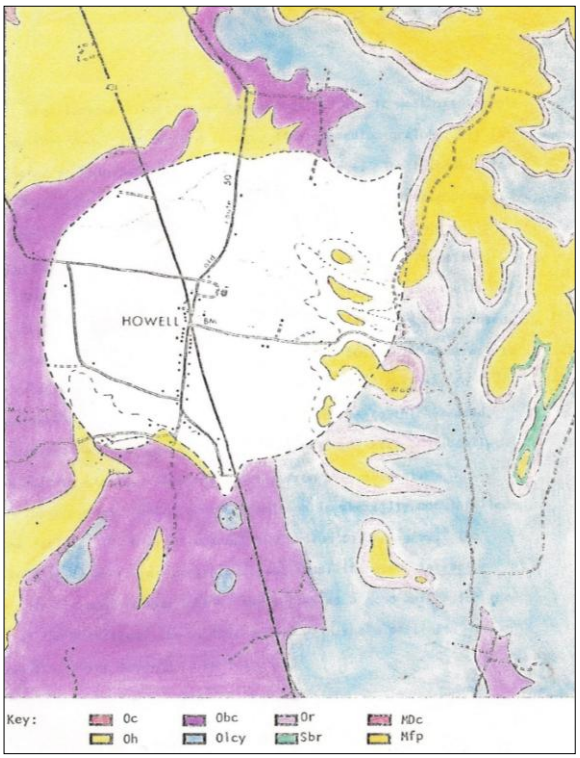

Figure 2: A geological map of the Howell region showing the area of deformation. Scale 1:24000 (after Woodruff, 1968).

2 HISTORICAL CONTEXT

Mr J.W. Young, of Fayetteville, Tennessee, ~10 km from Howell, was the first to notice this interesting, but "… small area of intricate structure …" (Born and Wilson, 1939: 371). He showed the Howell Structure to several geologists and discussed it with others, including Wilson and Born, sometime around 1934. As a result, the first known detailed map of the Structure and surrounding area was completed in 1937 by Born and Wilson. However, they did not come to a conclusion as to its origin, merely stating that

> While no conclusive evidence has been observed to support either the cryptovolcanic or the meteoritic hypothesis of origin of the Howell structure … [it] is considered tentatively as an example of the cryptovolcanic structures as interpreted by Bucher … (ibid.).

Detailed geological mapping of this area was undertaken again from 1964 to 1965 by Wilson and R.H. Barnes from the Tennessee Division of Geology, assisted by R.A. Miller and C.E.L. McCary (Deane et al., 2004; Woodruff, 1968). Figure 2 is the map prepared by Wilson and Barnes, with additions by C.M. Woodruff (1968).

The next serious study of the Howell Structure was undertaken in 1967 by Woodruff and supervised by R.G. Stearns, in order "… to map in detail the limits of deformation …" (Woodruff, 1968: 1). Woodruff (ibid.) noted that

> At the same time, geologists of the National Aeronautics and Space Administration began to do field reconnaissance work in preparation for core drilling to determine the nature of the structure at depth …

The lead geologist was J. Bensko, from NASA's Marshall Space Center in Huntsville, Alabama.

In late 2003 B. Deane, P. Lee, K.A. Milam, J.C. Evenick, and R.L. Zawislak carried out a study of the Howell Structure, including an aerial survey, in order to locate "… evidence of shock metamorphism in local lithologies …" (Deane et al., 2004: 1–2).

Finally, in 2015 Milam et al. published the results of their investigation of cores drilled by NASA scientists in the 1960s and limestone breccia samples supplied by R.G. Stearns. Through these new lines of investigation they were able to assemble what we regard as strong, but not conclusive, evidence for the impact origin of the Howell Structure.

3 MORPHOLOGY, STRATIGRAPHY, AND AGE

When he carried out his study, Woodruff (1968: 57) regarded the Howell Structure as a suspected site of impact, since its "… original morphology has been completely obliterated by the various geologic processes that have worked on the area …" The stratigraphy of the Highland Rim in which the Howell Structure is located is

> … primarily composed of flat-lying limestones, dolomites, and shales, and to a much lesser extent, of cherts, siltstones, mudstones, and very fine-grained to conglomeratic sandstones. Strata range from Upper Ordovician to Lower Mississippian in age and contain several prominent unconformities … (Deane et al., 2004: 1).

Woodruff (1968: 6) found similar strata, and rock units that he encountered at Howell included

> … the Hermitage Formation of the Nashville Group of the Ordovician System, through the Fort Payne Formation of the Mississippian System.

Figure 3 is Appendix A from Miller (1974: 59) showing a composite stratigraphical section for Middle Tennessee which includes rock units essential to the understanding of the Howell Structure. Note that the Stones (Black) River Group which includes Carters Limestone and the Nashville (Trenton) Group which includes the Hermitage Formation, Bigby-Cannon Limestone, and Catheys Formation, are from the Middle Ordovician. The Richmond Group is not specified on this particular stratigraphic section, but according to the U.S. Geological Survey is in the Upper Ordovician and includes the Mannie Shale, Fernvale Limestone, Sequatchie Formation, and Arnheim Formation. The Brassfield Limestone is Lower Silurian. Shown between the Pegram Formation of the Middle Devonian and the Chattanooga Shale of the Upper Devonian is a major unconformity found throughout Middle Tennessee. The Fort Payne Formation is Lower Mississippian. Note that in United States common usage, the Carbonifeorus System is divided into the Mississippian (early Carboniferous) and Pennsylvanian (late Carboniferous). Unfortunately, rocks that are exposed on the surface and

> … extend beneath the surface throughout Tennessee and other areas of the east-central United States … are referred to by other names elsewhere. (Miller, 1974: 19).

These include the Nashville/Trenton and Stones River/Black River Groups. Woodruff (1968: 52) points out one difficult issue related to the Howell Structure: "One does not know how much of the entire stratigraphic section was actually present at the time of explosion." He states that there could have been as much as 90 additional meters of Silurian at the time of the event, which adds even greater uncertainty to our understanding of the Howell Structure (ibid.).

The Howell Structure is "… a small area of highly disturbed, contorted, and brecciated strata." (Born and Wilson, 1939: 371). After studying and mapping the area in detail, Born and Wilson (ibid.) provided the following description:

> The salient structural feature is a circular area of intensely deformed Black River [Ordovician] and Trenton rocks, which have been uplifted approximately 100 feet [30 meters] above their normal positions. This circular area is composed of jumbled blocks of limestone imbedded in a matrix of shatter breccia. The major deformation is believed to have been Post-Trenton and pre-Fernvale in age. Overlying the shattered strata is the Fernvale Formation, the relative thickness and lithology of which point directly toward deposition in a graded crater.

During their investigation, Born and Wilson (ibid) also determined that "The younger Silurian and Mississippian formations are relatively undisturbed." They did not mention the cave located in the northeastern corner of the disturbance, which was noted in 2003 by Deane et al. (2004).

Born and Wilson (1939: 375) describe the structural features of Howell in three parts:

(1) the underlying, intensely-deformed rocks, which include Black River and Trenton strata;
(2) the Fernvale Formation; and
(3) the Chattanooga Shale and Fort Payne Chert.

Their investigation indicated that the

> … first series is separated from the second by a marked nonconformity with maximum differential relief of 100 feet [30 meters] within ½ mile [0.8 km] … (Born and Wilson, 1939: 375).

The plane of the nonconformity coincided with the pre-Fernvale surface. Figure 4 shows the structural cross section of the Howell Structure, as determined by Born and Wilson (1939: 376).

Born and Wilson note that "The much brecciated rocks of Black River and Trenton age are limited to a circular area about 1 mile [1.6 km] in diameter …" (ibid.), and the strata of these groups occur in blocks that vary from small fragments up

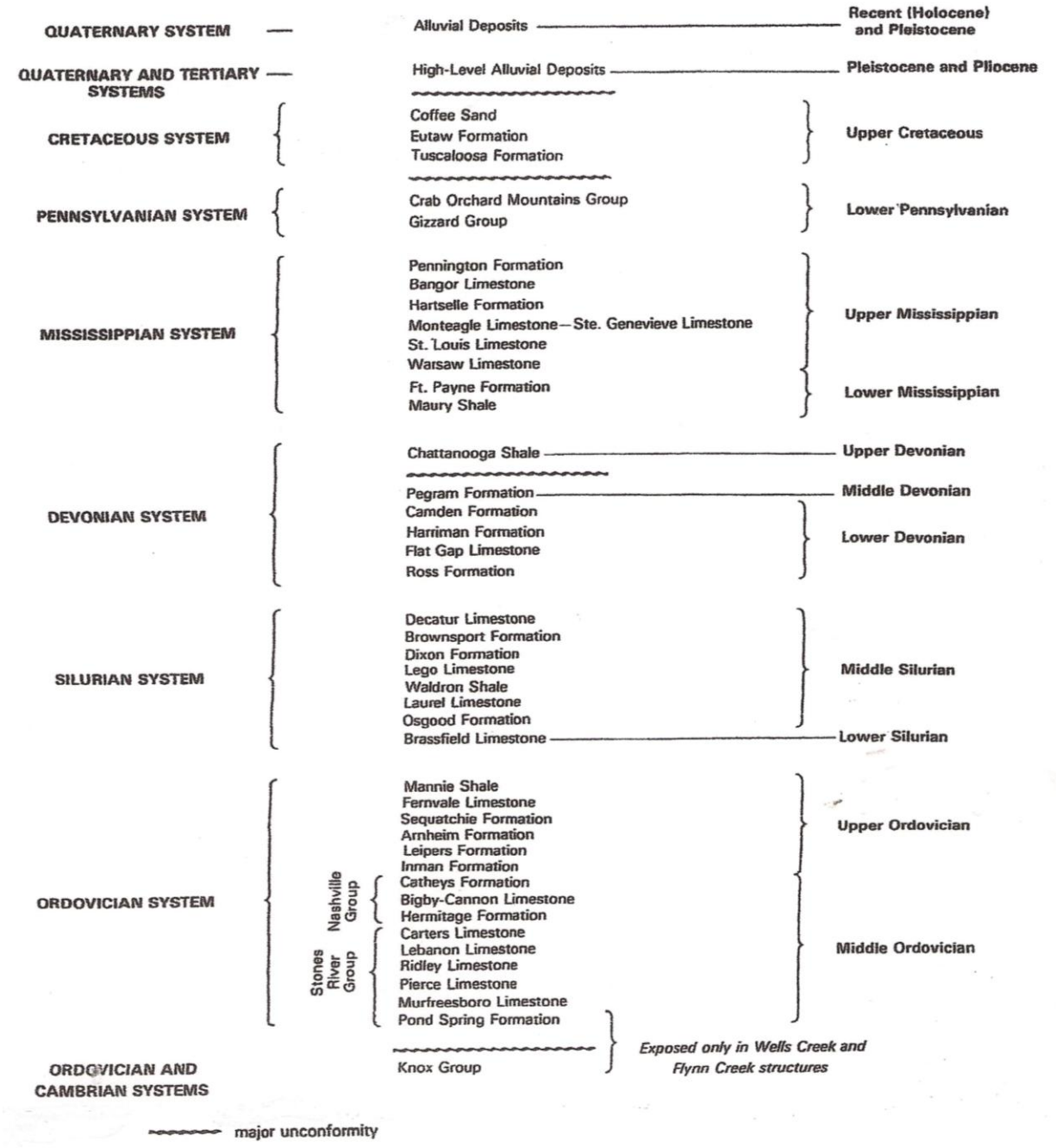

Figure 3: A composite stratigraphical section for Middle Tennessee (after Miller, 1974: 59).

to 20 feet [6 meters] or more. The blocks abut against each other at greatly-varying angles of strike and dip, with individual blocks showing

> … contortion and warping of bedding planes … [and] blocks of the Hermitage Formation have been rotated in respect to each other with resulting small-scale thrust-faulting … (ibid.).

This faulting, however, seems to be restricted to adjacent blocks that are in actual contact with each other:

> These blocks of limestone are imbedded in a matrix of shatter breccia composed of smaller fragments of limestone in a groundmass of powdered limestone. The breccia and the powdered limestone have been forced to flow around the blocks and along fractures within them, somewhat as in dike intrusion.

This circular area of jumbled, brecciated, and unbrecciated limestone has been uplifted vertically in part, so that blocks of Carters Limestone are now in juxtaposition with the surrounding undisturbed Cannon Limestone outside the brecciated area. The maximum uplift was approximately 100 feet [30 meters]. Some blocks of Trenton limestone occur at the same level, or even below, their normal horizon, but these blocks are believed to have fallen or rolled to these positions at the time of origin of the crater.

A rather definite break occurs between the

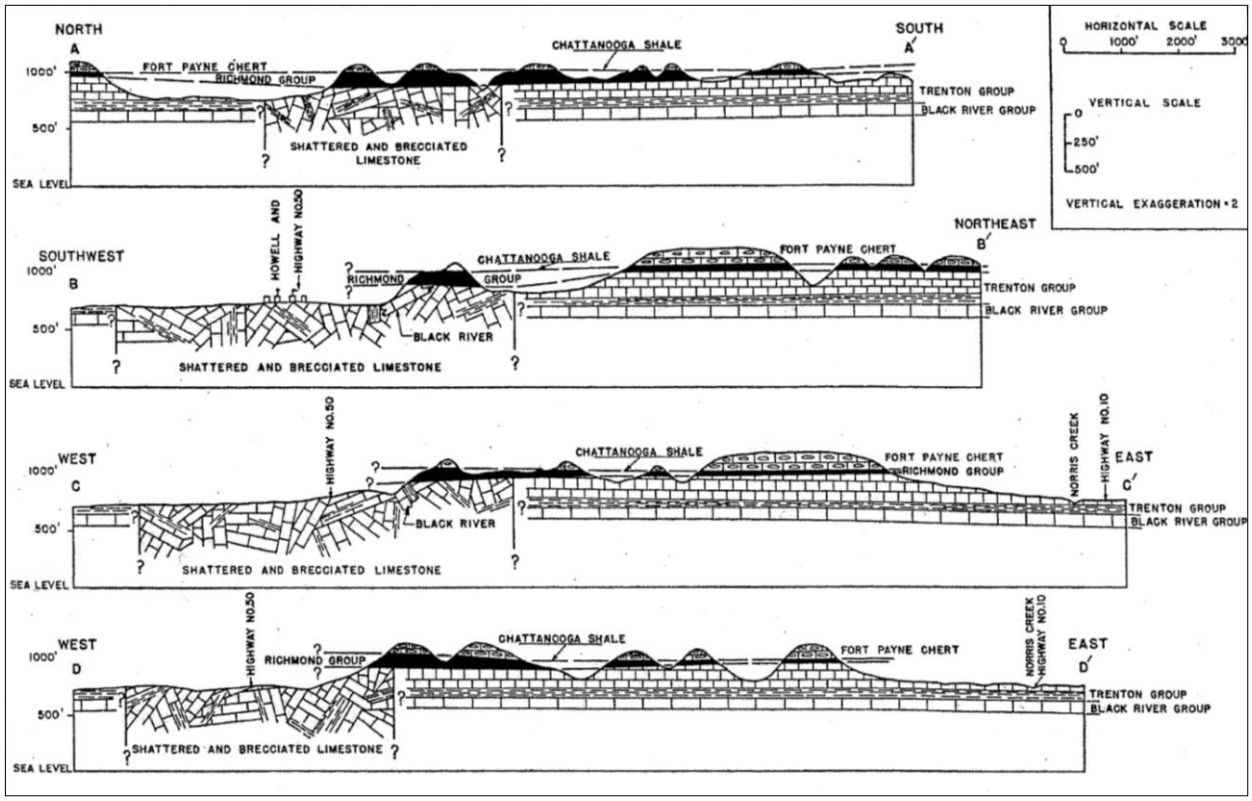

Figure 4: Structural cross-sections across the Howell Structure (after Born and Wilson, 1939: 376).

> jumbled and brecciated limestone within the circumference of the Howell disturbance and the surrounding normal limestone of the Cannon and Catheys formations.

Born and Wilson (1939: 376) note that "The Fernvale Formation rests nonconformably upon the underlying, greatly-deformed Trenton and Black River strata." However, the Fernvale Formation, is only preserved in the eastern section of the Howell Structure, as well as to the east of the disturbance, so its extensive removal "… prevents conclusive determination of its former extent, thickness, and structural details …" (Born and Wilson, 1939: 377). Mapping of the region that surrounds the Howell Structure shows that the Fernvale Formation is noticeably absent, indicating that its preservation in the disturbed area is "… due to unusual local conditions." (ibid.). Born and Wilson (ibid.) point out that

> … the rapid thickening of Fernvale from 15 to 115 feet [5 to 35 meters] toward the deformed area suggests some genetic relationship between the local abnormal thickness of Fernvale and the deformed area.

They conclude that a closed crater some 30 meters deep and 1.6 km in diameter existed in pre-Fernvale times. This 30 meter depth would be that of the crater at the start of the Fernvale deposition, so it can be inferred that the crater's original pre-erosion depth would have been greater:

> This crater must have been exposed to appreciable erosion before Fernvale deposition began, for its sides were not steep but rather were graded, as indicated by the abnormally thick Fernvale extending southeastward beyond the circumference of intense deformation that probably marked the limits of the crater. (ibid.).

The crater is thought to have filled with Fernvale sediments while flooded by the Fernvale sea (ibid.). The lower shale unit was not deposited for a long period of time, though, as "… the sea was soon freed from silt, and the clear-water limestone unit was deposited," (ibid.). Around 10 to 11 meters of this limestone unit were deposited before silt and quartz pebbles were subsequently brought in by the sea from a distant source. This last deposition completely filled the crater before the sea retreated.

The Fernvale limestone breccia is believed in part to have been the result of contemporary brecciation:

> One significant fact is that, even though locally brecciated, this limestone is a continuous unit that deposited over the strongly deformed rocks. Also, the elevation of the Fernvale limestone averages lower within the circular area of deformation than outside, where it overlies normal strata, indicating that the Fernvale did not participate in the uplift that locally raised rocks of the Black River and Trenton Groups above their normal levels. (Born and Wilson, 1939: 377).

The thick shale overlying this limestone locally has dips as great as 45°. Born and Wilson (1939) believe these dips are due to tilting and slumping that took place within the shale due to the settling and subsequent re-adjustment of the

underlying deformed strata. They also state, though, that

> … it may be necessary to postulate a mild post-Fernvale and pre-Chattanooga renewal of activity to account for such high dips … (Born and Wilson, 1939: 377).

It should be noted that if this subsequent activity was involved in the formation of the crater, then a meteoritic origin for the Howell Structure was not indicated. The overlying Chattanooga Shale and Fort Payne Chert formations show no brecciation, although they are warped, but Born and Wilson (1939) conclude that this warping had no relation to the pre-Fernvale crater.

Born and Wilson 1939: 377) state that the localized forces which brecciated the Black River and Trenton limestone

> … obviously operated after the deposition of the Catheys Formation… [but] As the Leipers Formation is not present today in this mapped area, it is impossible to date the brecciation relative to this formation … (ibid.).

They point out, however, that since

> … the Leipers Formation is believed to have covered most, or all, of central Tennessee … a post-Catheys, pre-Leipers crater should have been filled with Leipers sediments. (ibid.).

Born and Wilson (1939: 377–378) conclude that the age of the Howell Structure must be determined from the following restraints:

> Even though the Fernvale limestone unit is locally brecciated and high dips occur in the Fernvale shale unit, the major deformation, when viewed from a study of all known facts as well as these anomalies, would appear to have been pre-Fernvale. There is no basis for argument for a post-Fernvale date for the maximum deformation, but there is some basis for believing in a post-Fernvale renewal of the activity, which was so great in pre-Fernvale times. If this did occur, it would have an important bearing on the problem of origin of the deformative forces; but, unfortunately, the data are not sufficient to prove that the initial strong pre-Fernvale deformation was followed by a mild post-Fernvale renewal of deformation.
>
> In summary, it is believed that the major deformation in the Howell disturbance may be dated as post-Catheys (probably post-Leipers) and pre-Fernvale, with possibly post-Fernvale and pre-Chattanooga recurrence in a mild form.

Born and Wilson (1939: 380) note that

> If the Leipers formation were deposited prior to the explosion, as is believed to have been the case, it was removed by post explosion erosion. No evidence is available for dating the explosion with regard to the Arnheim Formation.

Summarizing their findings at the Howell site, Born and Wilson (1939: 380) state that an explosion occurred,

> … blowing out a crater at least 100 feet [30 meters] in depth and 1 mile [1.6 kilometers] in diameter, and piling up limestone debris around the crater … [Subsequent] Removal of this debris (and possibly the Leipers Formation from the surrounding area) and the grading of the crater walls by erosion … [occurred before] Deposition of the Fernvale Formation, filling the crater level with the surrounding floor of the Fernvale sea … (Born and Wilson, 1939: 380).

A 1961 United States Geological Survey, Branch of Astrogeology report includes the following entry:

> Field examination of the Howell disturbance, Tennessee, by E.M. Shoemaker, R.E. Eggleton, and D.J. Milton, in company with C.W. Wilson Jr. of Vanderbilt University, led to the conclusion that if this structure is of impact origin, as has been suggested by Wilson and others, the structure was probably formed at a time when the epi-continental Ordovician sea had significant depth at the site of the Howell disturbance. (Schaber, 2005: 31).

Woodruff (1968: 44–45) undertook the next major study of the area and mapped the Howell Structure's limits by including

> … all expressions of deformation beyond an established 'norm' as being within the structure … all dips greater than those of the normal regional dip, all fracturing, folding, faulting, overturning, and brecciation.

Woodruff (1968: 46) states that

> The structure limits cannot be interpolated with ease from any one point to another. Interpolation is necessary, even though undesirable, in some areas because of lack of outcrops.

Woodruff (1968: 46–47) determined that the Howell Structure was roughly circular and somewhat irregular in outline, as shown in Figure 2. In locations where the Structure's boundaries seemed to deviate from an idealized circular outline, Woodruff (1968: 49) believed that the

> … deviation might be due to dip of the structure at depth, which would give an irregular trace conforming to topography. Such irregularities might also be due to the vicissitudes of shock in rock layers at depth.

He also determined that Howell is "… slightly elliptical with the axis of the ellipse trending slightly northeast …" (Woodruff, 1968: 47). The Structure's minor axis is around 1.8 km and trends north-south, while the major axis is about 2.5 km and trends approximately north 45 degrees east. Woodruff did not find an appreciable uplift between the rock units within the Howell Structure and the surrounding undisturbed strata, although he did suggest further investigation in order to verify this finding.

Woodruff (1968: 50) constructed an idealized cross-section of the Howell Structure by assum-

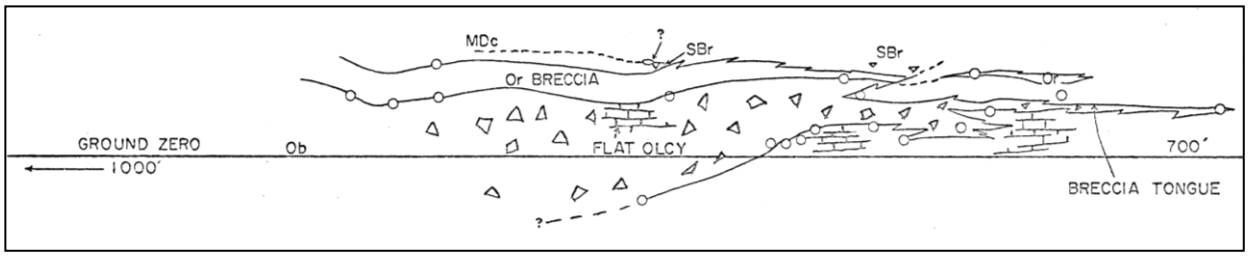

Figure 5: An idealized cross-section across the eastern half of the Howell Structure assuming radial symmetry. The series of small circles are control points (after Woodruff, 1968: 51).

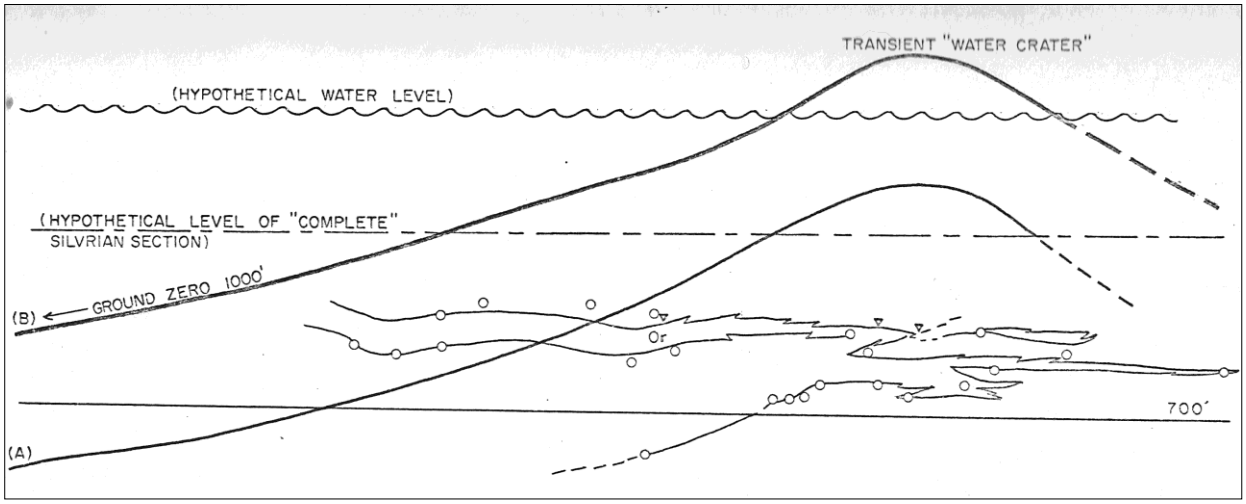

Figure 6: Two hypothetical Howell half-craters superimposed on the idealized cross-section across the eastern half of the Howell Structure. (A) assumes 300 feet of Silurian strata to have been present, and (B) assumes 400 feet of water above these Silurian strata (after Woodruff, 1968: 55).

ing that the Structure possesses "… basic radial symmetry …" and by utilizing "… topographic elevations of the outcrops …" from his compilation map. The eastern half of his cross-section is seen in Figure 5. Woodruff (ibid.) notes that as with the surface boundaries, the resulting drawing shows irregular deformation limits at depth, and he discusses the implications:

> This irregularity could be an artifact of the projection technique, but may well be real and due to a propensity of shock to be transmitted along bedding planes, or at least parallel to bedding. The irregularity may be due to the vagaries in behavior of different lithologic types when subjected to such forces … Only extensive subsurface information will demonstrate whether such boundaries actually exist. (ibid.).

If Woodruff's idealized cross-section is correct, then "… the zone of deformations is not as deep as would be expected …" (ibid.), but Woodruff (1968: 52) does note that "One does not know how much of the stratigraphic section was actually present at the time of explosion." Based on the complete Silurian section found in the Western Valley of Tennessee, there may have been as much as 90 meters of Silurian strata present at the time of the Howell event. Another possibility is that Howell "… at the time of impact (or explosion) was under water …" (ibid.). Figure 6 shows the eastern side of the idealized cross-section by Woodruff (1968: 55), with two superimposed half craters assuming (a) 90 meters of Silurian strata and (b) 90 meters of Silurian strata under another 120 meters of water. Woodruff (1968: 57) continues:

> … the depth of water would be equivalent to a certain amount of rock in dissipating the shock. At the same time, no indication of deformation would remain in water after the event …

Woodruff noticed a 'gradation zone' from 18 to 45 or so meters between the breccias and normal, undisturbed rock as he mapped stratigraphic units from " … normal flat-lying beds into zones of intense deformation …" (Woodruff, 1968: 45). "This same relationship seems to hold true in subsurface work …" according to a personal communication between Bensko and Woodruff (1968: 3, 45) regarding the Howell core which was drilled by a crew from the National Aeronautics and Space Administration's Marshall Space Center located in nearby Huntsville, Alabama. Most of the questions concerning the Howell Structure's limits of deformation at depth require subsurface data which Woodruff (1969: 49) points out are not extensive since such data requires

> … drilling into a section of deformed rock and continuation of the drilling until undisturbed rock layers are reached … only one such NASA drill hole was available …"

Bensko informed Woodruff

> … that the drill hole penetrated past the breccias into undisturbed bedrock, and that there was a zone of gradation between the breccias and the normal bedding … (Deane et al., 2004: 2; cf. Woodruff, 1968: 65).

According to Woodruff (1968: 57),

> Essentially, all geomorphological indications of deformation are expressed in joint, and/or fault controlled stream lineations and joint and fault control of escarpments …

and he cites several striking examples of joints controlling the stream pattern within the Howell Structure:

> Cane Creek turns about 80 degrees, reflecting a joint pattern radiating outward from near the center of the structure. Again on Cane creek, but outside the northwestern limits of the structure, is another such elbow turn, where the joint similarly appears to radiate outward from the center of the structure. Striking joint control is further seen in the tributary of Cane Creek that cuts the northern portion of the structure … The joint pattern again appears to radiate.
>
> These features indicate an event of sufficient magnitude to give rise to a more or less radiating set of joint fractures in surrounding otherwise undisturbed rocks. (ibid.).

This finding rules out localized sedimentary processes that would have caused slumping and brecciation. Other geomorphological indications of structure according to Woodruff are also joint and/or fault controlled within the area of deformation. These are

> … the apparent alignment of the dissected escarpments on the eastern ridges making up the drainage divide between Cane and Norris Creeks … (Woodruff, 1968: 58).

He notes that these features also radiate from a central area in the Structure.

Woodruff (1968: 23) discusses the age of the Howell Structure based on stratigraphical relationships:

> On the western two-thirds, erosion has cut deep into the roots of the structure completely obliterating most geomorphological indications of deformation. However, on the high ground on the southern and eastern side, the structure is buried by undeformed Fort Payne chert of Mississippian age. This is valuable because it limits the structure to a pre-Fort Payne time of origin. However, certain problems have arisen in dealing with rock units older than Fort Payne.

In his discussion, Woodruff (1968: 23) notes that Born and Wilson recorded the finding of strong dips, local faults and some brecciation in the Richmond Group of rocks at Howell and "… that the geologic sequence of events was further confused by the presence of tongues of the Fayetteville channel of Richmond Age." He then explains how he arrives at an age for the Howell Structure:

> Born and Wilson (1939) placed the age of the structure as being post-Leipers and pre-Richmond. The fact that the Richmond Group occurs as a continuous belt of rocks (and can be mapped as such) overlying the much more intensely brecciated older Ordovician rocks and the fact that this belt of Richmond contains only blocks and fragments of Richmond (never blocks of older Ordovician age) led them to this conclusion. They attributed the deformation of the Richmond to contemporaneous brecciation that occurred shortly after the partial consolidation of the Richmond as a result of readjustments in the underlying jumbled breccia of older Ordovician rocks and also to a possible mild renewal of the forces that caused the original major deformation (volcanic origin required for this).
>
> The present writer has now asserted that the age of the structure is definitely post-Richmond – indeed post-Silurian, on the strength of the discovery of brecciated lenses of chert, identified by Wilson as being in the Brassfield Formation (Silurian). Also, another zone, which may represent an intensely deformed area of still younger age, has been found by this writer. This consists of a mixed zone of chert, sand, various sulfides, and possibly even carbonaceous shale material. Petrographic study shows planar features cutting across quartz grain boundaries, and the possible presence of glass, and/or isotropized quartz. The zone has been postulated by Stearns as being a mixture of Silurian (Brassfield) and Devonian (basal sand of the Chattanooga Shale). The most realistic appraisal of a "normal" stratigraphic position for the so-called "mixed zone" would be in the basal sand of the Chattanooga Shale. This still gives a striking parallel in time of deformation with the Flynn Creek structure. (Woodruff, 1968: 23, 27).

Woodruff (1968: 28) concludes that the age of the Howell Structure

> … may be stated with authority as being post-Brassfield, and possibly into the upper Devonian time … Also, it is safe to say that the structure is pre-Fort Payne.

A possible explanation of the 'mixed zone' discussed above "… is that it may be the fossilized crater rim, buried and thus preserved from erosion by the Fort Payne chert." (Woodruff, 1968: 27). The possibility that this 'mixed zone' may be composed of rim material is indicated by petrographic studies, and based on samples that are possibly reworked rim material Woddruff (1968: 63–64) concludes:

> It contains fragments from Brassfield chert, and basal sand of the Chattanooga Shale. The quartz grains that are deformed are probably of Devonian age, probably from the

> basal sand member, but it is believed that the Chattanooga Shale is post-deformation in age. This gives the outstanding age control that was hoped for from the beginning. The age can be bracketed into a time zone in the uppermost Devonian. It is known to be pre-Fort Payne (Mississippian), and is probably pre-Chattanooga (Devonian-Mississippian). This means that the Howell event could exactly coincide with the Flynn Creek structure in age, as the Flynn Creek crater is filled with material of Chattanooga age…
>
> The rock units exposed in the Howell area range from the Hermitage Formation of Ordovician age to the Fort Payne Formation of Mississippian age. The units involved in the deformation range from the Hermitage through the Brassfield of Silurian age. Another younger rock unit, considered to be a mixed zone between Silurian and Devonian and Mississippian units was found. Constituent members of that rock unit were also deformed. The geological age of the structure has been placed as certainly post-Lower Silurian and probably post-lower Devonian. It is probably pre-Chattanooga and is certainly pre-Fort Payne Chert (Mississippian).

In another discussion of the age of the Howell Structure, Miller (1974) points out that the adjacent Fort Payne rocks, which are Lower Mississippian, are not structurally disturbed, indicating that the Structure's origin is pre-Mississippian and that Silurian rocks in the Howell Structure are brecciated, indicating it is post Silurian. Miller (1974: 56) also compares the Howell Structure's age to that of Flynn Creek, a confirmed impact site in Tennessee, noting that Flynn Creek "… formed in Middle to Late Devonian time (350–375 million years ago), for it is filled with Chattanooga Shale …" Miller (ibid.) concludes that

> … the Howell Structure may be very close in age to the one at Flynn Creek, or some time in the Devonian Period, possibly just prior to deposition of the Chattanooga Shale …

Miller also notes that Howell, unlike the larger Flynn Creek and Wells Creek impact structures in Tennessee, is only 2.1 km in diameter and that there are some dissimilarities between this and the other Tennessee impact sites. He points out that

> There is no distinct central uplift, although intense brecciation and other disturbances of the rocks have possibly concealed or obliterated an otherwise more definitive uplift … (ibid.).

However, on the Earth the transition from a simple to a complex crater occurs around a diameter of 2 km in sediments and 4 km in massive crystalline rocks (French, 1998: 24). Howell might just be a simple crater and as such would not possess a central uplift.

Miller (1974: 56) also states that "Although there are faults within the Howell Structure, there are no clearly definable circular faults surrounding it …" However, we dispute this, as there are three more or less parallel faults to the southwest of Howell that are seemingly centered on the Structure, and although there is no published information that would suggest that the faults are in any way associated with the Howell Structure, their proximity to it is interesting. The distances of the faults from the Structure, as measured on a 1:250,000 map, are approximately 6.4, 22.5, and 38.6 kilometers, but they are not concentric to the Howell Structure, and since they are situated on the S-SW periphery of the Nashville Basin another possibility is that they may have been formed during the uplift of the Nashville Dome, and thus are related to that structure. If this was so, their proximity to the Howell Structure may merely be coincidental. Figure 7 shows a generalized tectonic map of the southern interior lowlands of the United States, and includes the Howell Structure, the three faults and the Nashville Dome.

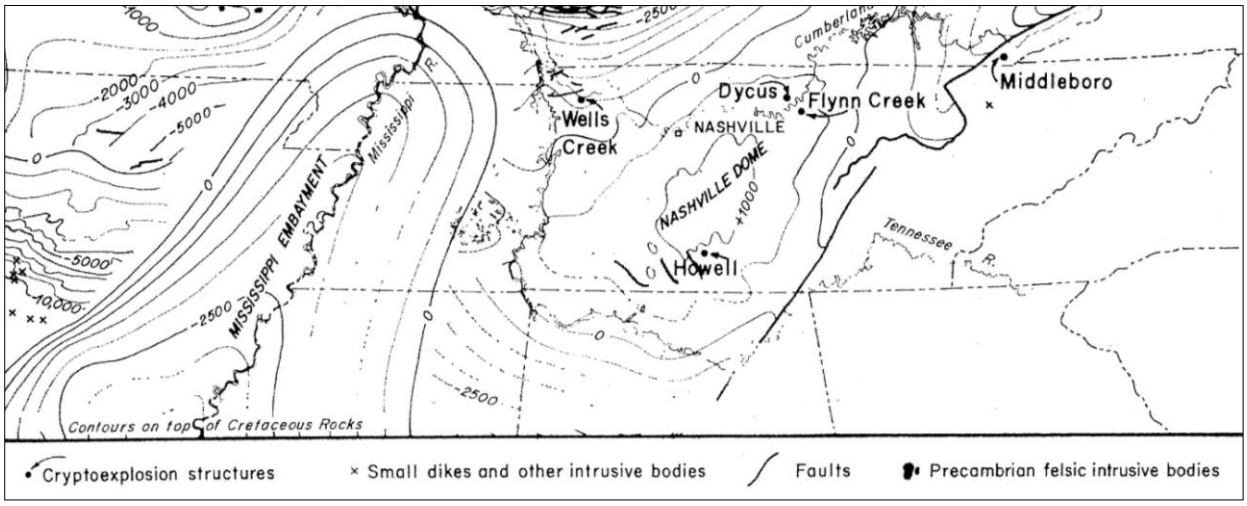

Figure 7: A generalized tectonic map of the southern interior lowlands of the United States which shows the locations of the Howell Structure and the Nashville Dome with respect to the three concentric faults (after Roddy, 1968: 293)

4 CRATERING MECHANICS

As Croft (1977: 1279) points out, "Impact cratering, an extremely complex phenomenon worthy of study in its own right, acquires great significance when studied in the context of planetary surfaces and planetary formation …" After decades of controversy, a modern understanding of the high energies associated with impact cratering finally led investigators to the realization that impact crater excavation is similar to an explosion (Hoyt, 1987; Melosh, 1989). We now have a good idea of the basic cratering process.

Let us now examine this for a terrestrial (rather than a marine) non-oblique impact, so that we can determine features of the initial impact and the form of the crater that is now represented by the Howell Structure (on the assumption that it is a highly-eroded meteorite impact scar). There are four different aspects to consider, and these are discussed separately below.

4.1 Impact Velocity and Energy

The Earth's atmosphere provides protection against small meteorites, but is no match for the more massive ones which enter the atmosphere carrying large amounts of kinetic energy. Loss of mass due to ablation depends on a meteoroid's composition, size, mass, altitude, and entry velocity. The density of Earth's atmosphere varies from 10^{-13} g/cm^3 at an altitude of 200 km to 10^{-3} g/cm^3 at ground level and meteoroids entering the Earth's atmosphere have masses ranging from ~10^{-18} to ~10^{15} kilograms (Popova, 2005). Meteoroids larger than ~100 m and ~10^9 kg lose only a small part of their initial mass and energy while traveling through the atmosphere.

The sufficiently-massive cosmic bodies are not significantly slowed by friction in the Earth's atmosphere and so impact the ground at cosmic velocities, typically tens of kilometers per second (French, 1998). The maximum possible impact velocity of an impactor gravitationally bound to the Sun is 72 km/sec (Collins et al., 2005). However, the average asteroidal impact velocity on Earth is 17 km/sec (Collins et al., 2004). A meteorite's kinetic energy changes with the square of its velocity. This energy is released upon impact and, if sufficiently high, will result in an explosion. Even if a meteoroid does not survive to impact the Earth's surface, but instead explodes in the air low over the Earth's surface, powerful shock waves and radiation fluxes can still occur which may result in fires, and the destruction of objects on the Earth's surface (Nemchinov et al., 1999).

For large meteoroids, ablation from the surface is not significant because of shielding by the vapor produced and so the mass of the meteoroid or its fragments changes little with fragmentation (ibid.). Modeling indicates that the size of a dense vapor cloud formed around a meteoroid is around 5–10 times its size (Popova, 2004: 311). Vapor parameters depend on the meteoroid's size, velocity, altitude and composition. According to Nemchinov et al. (1999), the actual velocity, V, including atmospheric retarding effects, of a meteoroid of mass M, with cross sectional area S, at a height of Z_r below the defined atmosphere Z (where Z = 0 at the Earth's surface), where the expected velocity is V_r, for a trajectory of angle θ, is given by:

$$V^2 = V_r^2 \exp^{[-m_a I m_0 \sin\theta]} \quad (1)$$

where C_D is the drag coefficient and the effective mass per unit of area of the meteoroid is found by $m_0 = M/SC_D$. In the exponent, the mass of the atmospheric column per unit area, m_a, is defined by the integral of the density of air, ρ_a, so $m_a(Z) = \int_Z^{Z_r} \rho_a dZ$ (Nemchinov et al., 1999: 1196). Retardation begins where the specific mass of the atmosphere becomes comparable to the specific mass of the meteoroid.

Blast waves generated by high-velocity meteoroids in the atmosphere are similar to shock waves generated by a line charge (Ivanov, 1991). The blast wave generated during the 1908 Tunguska event when a meteoroid, perhaps a comet, decelerated and exploded above Earth's surface rather than impacting it, starting a forest fire and felling trees in a 50 × 60 km area in central Russia. For a high-velocity meteoroid, the distance scale of its atmospheric blast/shock wave, λ, can be found by:

$$\lambda = [\eta(e/P_a)]^{½} \quad (2)$$

where P_a is the ambient atmospheric pressure, e is the energy of the explosion or deceleration per unit length of the trajectory, and η is the efficiency of the transformation of this energy to blast waves. For high-velocity bodies, η = 2 (ibid.). Shock vapor is produced by a high-velocity impact. Expanding shock vapor in turn generates atmospheric shock waves. If impact velocity is greater than 30 km/sec for a projectile impacting 'typical igneous rock', then the mass that is vaporized may be found by:

$$M_V = 0.05\, E \quad (3)$$

where M_V is the mass of the vapor and E is the kinetic energy of the impactor in units of TNT equivalent (ibid.).

Meteoritic material strengths and densities differ from one meteorite to another and even within one body. Strengths of different pieces of the same meteorite can differ by a factor of 2–3 correlating weakly with the meteorite's chemical-petrological composition (Nemchinov et al., 1999). The surprising result is that some stony meteorites are stronger than some iron meteorites. Also, the strength of a large meteoroid or its fragments is lower than the strength of the

small specimens on which experiments are made. The characteristic loads for which bodies of mass M break up in the atmosphere is lower than the strength limits of the small specimens of a meteorite σ_s of mass $m_s << M$. The variation of strength of a meteoroid of mass M can be found by:

$$\sigma = \sigma_s (m_s/M)^{\alpha} \quad (4)$$

where α is determined by the degree of homogeneity of a body. The more homogeneous a meteoroid is, the smaller α will be, with a good estimate being α = ¼ (Nemchinov et al., 1999). However, if α is established on specimens of different dimensions in the range of 1–10 cm, extension of dependence to bodies with dimensions of 1–100 m can result in significant errors.

A terrestrial meteorite impact crater is not formed by the impact itself, but by the blast of "… superheated, compressed air and other vaporized matter." (Baldwin, 1949: 135).

> The known terrestrial meteorite craters were all blasted into being by the almost instantaneous release of the kinetic energy of motion of the [impacting] mass. (Baldwin, 1949: 68).

According to Baldwin (1949: 97) the few relatively modern meteorite impact craters recognized on Earth show evidence of "… tremendous explosive activity …" including the radial distribution of explosively-shattered meteorite and target rock fragments as well as blocks of target material spread over an area ten times the resulting crater's radius.

An impact crater's radius and depth depends on the energy of impact as well as the density, composition, and size of the impactor and the surface composition and gravitational acceleration of the planet (de Vet and de Bruyn, 2007; Masaitis, 2005). Surprisingly, de Vet and de Bruyn (2007) found that when a spherical projectile is dropped vertically into a container of granular material, glass beads, the excavation energy required for crater formation is only a small fraction (0.1%–0.5%) of the projectile's kinetic energy. For a flat surface defined to have the vertical coordinate z = 0, so that a crater's interior has z < 0, the excavation energy, E_x, required to eject the crater volume out of the crater and deposit it on the surrounding surface is given by:

$$E_x = \pi \rho_b g \int_0^R z(r)^2 r \, dr \quad (5)$$

where ρ_b is the bulk density of the granular material, r is the radial distance, and R_0 is the crater's radius at z = 0. While both are dependent on impact energy, a crater's radius depends on the projectile size, and depth depends on projectile density. The rim height was found to depend only on the projectile's size (de Vet and de Bruyn, 2007).

The mass of the meteorite needed to account for a given impact crater is inversely proportional to the striking velocity of the meteorite. As a meteorite penetrates Earth's layers, it initially moves faster than the impact-induced shock waves, compressing an ever increasing amount of target rock. This material combined with the meteorite's mass will slow rapidly, but momentum will be maintained as the combined mass increases. Baldwin (1949: 139) states that "Essentially no momentum will be lost during this interval …" Momentum is the product of the mass and velocity of an object, therefore a higher-velocity meteorite will form a larger crater than a meteorite of equal mass moving at a lower velocity.

In hypervelocity impact experiments carried out on low density materials, the penetration track of the projectile becomes longer as the target medium density is lowered (Kadono, 1999). At low impact velocity, V_0, the strength of a projectile, Y_p, is greater than the dynamic impact pressure, so the projectile penetrates the target intact and the resulting crater is narrow and deep. Assuming a spherical projectile of diameter D_p, and density ρ_p, collides vertically with a surface having target strength, Y_t, and target density, ρ_t, and the initial impact pressure, P_0, is low enough for the projectile to remain intact after target penetration, then according to Kadono and Fujiwara (2005: 1311), the resulting crater depth/projectile diameter ratio, T/D_p, can be determined by:

$$T/D_p \sim (⅓)(\rho_p V_0^2/Y_t) \quad (6)$$

With increasing impact velocity, the point at which the initial impact pressure, P_0, equals Y_p, the deformation or fragmentation of the projectile begins (Kadono and Fujiwara, 2005). As the impact velocity is further increased, the projectile shatters and penetration depth decreases. If the initial impact pressure, P_0, is higher than the projectile strength, Y_p, then the situation is similar to cratering with chemical explosives. Where U_p is the shock wave velocity, C_{Rp} is the rarefaction velocity, and α is the attenuation rate of pressure, the crater depth/projectile diameter ratio, T/D_p, becomes:

$$T/D_p \sim (\rho_p/\rho_t)(P_0/Y_p)^{1/\alpha}(Y_p/Y_t)^{1/\alpha} \ln [1+ (\rho_t V_0/\rho_p)(1/U_p + 1/C_{Rp})] \quad (7)$$

Numerical simulations show α ~3 for high velocity impacts and experimental values obtained give α ~2–3, which is not surprising since this cube-root scaling form is often realized in chemical explosive cratering (Kadono and Fujiwara, 2005: 1312). After impact, strong shocks propagate into the target and projectile which brings them to a common pressure P (Melosh, 1989: 54). The rarefaction wave speed, C_{Rp}, can be found by:

$$C_{Rp} = [(K_0 + nP)/\rho_{Cp}]^{½} \quad (8)$$

where the projectile bulk modulus is $K_0 = \rho_{0p}C_p^2$ and $n = 4S_p - 1$ utilizing the uncompressed density of the projectile, ρ_{0p}, the compressed density of the projectile, ρ_{Cp}, and empirically determined parameters of the projectile material C_p and S_p. This same equation can give the rarefaction speed in the target if the target's parameters C_t, S_t, and ρ_{0t} are used instead. For an iron projectile impacting a Gabbroic anorthosite target, C_t = 7.71 km/sec, S_t = 1.05, ρ_{0t} = 3.965 Mg/m^3, C_p = 4.05 km/sec, S_p = 1.41, and ρ_{0p} = 7.8 Mg/m^3 where S is dimensionless (Melosh, 1989: 56–57).

Shoemaker (1983) utilized data from the Jangle U nuclear crater in Yucca Flat, Nevada, USA, in the following equation used to determine the diameter, D_t, of a terrestrial impact crater.

$$D_t = c_f K_n (W\rho_a/\rho_t)^{1/3.4} \quad (9)$$

In this equation, the kinetic energy of a projectile of diameter d, density ρ, and velocity v, all measured in cgs units, is represented by $W = (^1/_{12})(\pi d^3 \rho v^2)/(4.19 \times 10^{10})$ kilotons TNT equivalent. The scaling coefficient, K_n = 0.074 km kilotons$^{-1/3.4}$, is an empirical constant derived from the diameter and explosive yield for the Jangle U nuclear crater. The estimated density of the alluvium at the Jangle U site is ρ_a = 1.8 g/cm^3 and ρ_t is the mean density of the target rocks. The crater collapse factor, c_f, is considered to be 1 for craters with diameter ≤3km and 1.3 for craters with diameter ≥4 km. Shoemaker considered 30% to be a conservative estimate for the diameter enlargement of an impact crater due to wall collapse

When these large quantities of energy are released quickly and close to Earth's surface, a rapid and orderly series of events is initiated that will result in an explosion crater. This process is continuous but can be divided into three main stages: contact and compression, crater excavation and material ejection, followed by modification of the transient crater (Gault et al., 1968; French, 1998; Melosh, 1989). Craters at the end of the excavation/ejection stage are unstable due to the steepness of their walls and experience some modification due to collapse, so craters at this stage are referred to as transient craters. Transient craters will experience initial modification to the 'final' crater form as well as continued modifications that are due to normal geological processes (French, 1998). The area of destruction due to impact is much smaller than the size of the final crater due to the modifications which start almost immediately after impact (ibid.).

4.2 Contact and Compression

The first stage begins when a meteorite makes contact with the target surface and compresses it creating shock waves through conservation of energy (French, 1998). High pressures develop along the interface as the target rock's resistance begins to decelerate the impactor. A hemispherical shock front spreads and propagates during the time that the meteorite's initial kinetic energy is transferred to the target rock, which is compressed, distorted, heated and accelerated (ibid.).

Immediately after initial contact, two shocks actually propagate away from the meteorite-target interface, one reflected back into the impactor and the other downward into the target material (ibid.). By the time the impactor and target interface has reached a depth of approximately one-half of the impactor's original diameter, the meteorite itself is engulfed by the shock wave which is in turn reflected as a rarefaction or release wave when it reaches the meteorite's rear surface. A free surface cannot sustain a state of stress, so a rarefaction wave allows for decompression from the high pressure state behind the shock wave to ambient pressure (Gault et al., 1968). Unloading to near zero pressure from the high pressures created during compression may cause both the meteorite and target rock to melt or vaporize (French, 1998). As the shock waves travel through target rock and their velocity drops to that of sound, 5–8 km/s, the shock waves become elastic or seismic waves (ibid.). Weak disturbances produce elastic waves in solids or sound waves in liquids. Stronger disturbances cause plastic waves and irreversible deformation in the solids through which they travel. The strongest disturbances produce shock waves which travel faster in uncompressed material and are, therefore, supersonic (Melosh, 1989).

The relationships between parameters across a shock were derived by P.H. Hugoniot in 1897. His equations, along with the equation of state, are used to model the impact cratering process (Pierazzo and Collins, 2003). The Hugoniot equations use the conservation of mass, momentum and energy across a shock front to relate the density ρ, pressure P, and internal energy per unit mass E, in front of the shock wave to the values of these same variables after the shock wave has passed (Melosh, 1989). The reference frame is usually chosen so that the unshocked material is at rest and shock velocity, U, and particle velocity, u_ρ, are unknown. Density is sometimes expressed as specific volume $V = 1/\rho$. For initial density ρ_0, pressure P_0, and internal energy E_0, conservation of mass leads to the first Hugoniot equation:

$$\rho(U - u_\rho) = \rho_0 U \quad (10)$$

Conservation of momentum leads to the derivation of the second Hugoniot equation:

$$P - P_0 = \rho_0 U u_\rho \quad (11)$$

Conservation of energy leads to the third Hugoniot equation:

$$E - E_0 = (P + P_0)(V_0 - V)/2 \quad (12)$$

An equation of state relates the thermodynamic variables for pressure, density or specific volume, and specific internal energy or temperature T. As Melosh (1989: 230) notes,

> The equation of state is different for different materials and is a complex function of the molecular and atomic structure of the given substance.

The response of a given material to an impact shock is governed by its equation of state since the above Hugoniot equations are the same for all materials (ibid.). The Tillotson equation of state was derived specifically for high-velocity impact computations and also has parameters which allow for the description of unloading of shocked material into the vapor phase (ibid.). The first form of the equation, used when material is compressed to higher density than its zero-pressure form, $\rho/\rho_0 \geq 1$, and the energy density, E, is less than the energy of incipient vaporization, is:

$$P = [a + b/(E/(E_0\eta^2) + 1)]\rho E + A\mu + B\mu^2 \quad (13)$$

In this equation $\eta = \rho/\rho_0$ and $\mu = \eta - 1$. The Tillotson parameters are a, b, A, B, and E_0, however, E_0 is not the initial energy density, it is a parameter often close to the vaporization energy (ibid.). The parameter a is usually equal to 0.5 based on observational data. The second form of the Tillotson equation is utilized when material is expanded to lower density, that is $\rho/\rho_0 \leq 1$, and internal energy exceeds the energy of complete vaporization. Here, the pressure is found by:

$$P = a\rho E + \{b\rho E/(E_0\eta^2) + 1) + A\mu e^{-\beta(\rho_0/\rho - 1)}\} e^{-\alpha(\rho_0/\rho - 1)^2} \quad (14)$$

The constants α and β control the rate of convergence of this second equation to the perfect gas law (ibid.).

Contact and compression is the shortest stage of the impact cratering process. At the point of impact, the Earth itself offers strong resistance to meteoritic penetration, so a meteorite's rate of deceleration is quite rapid, and

> Even the high-velocity meteoritic masses moving more rapidly than the velocity of shock waves in the earth's crust must be brought to rest within a very small fraction of a second. (Baldwin, 1963: 9).

Moreover,

> The contact/compression stage lasts no more than a few seconds, even for impacts of very large objects … For most impact events, the entire contact/compression stage is over in less than a second … (French, 1998: 19).

This stage ":… lasts a second or more only for the very largest impacts …" (Melosh, 1989: 46), and its duration is given by:

$$\tau = L/v_i \quad (15)$$

where v_i is the meteorite's initial velocity and τ is the time required for the impactor to travel through the target rock a distance equal to its diameter L in a vertical impact. Note that $v_f = 0$.

The kinetic energy of a high-velocity meteorite that is transformed into compression waves and heat energy may be practically unlimited, although most of the meteorite's kinetic energy is stored in the compressed rock rather than transformed into heat. According to Baldwin (1963: 69–70) during an impact event,

> … much of the energy is transmitted in shock waves through the crust and air and thence gradually converted into heat [and] … It is only after the velocity drops below that of the shock waves that the phenomenon of heat enters the picture.

Estimates are that around "… 25–50% of the projectile's original kinetic energy was converted into heat …" during the Chicxulub impact event (French, 1998: 8). Hot rock may be buried, though, at a depth that is as great as the final crater depth. Melt layers near the surface would cool quickly, but the cooling time for deeply-buried layers would be much slower. "Melt in the breccias lens underlying a 15-km diameter crater is thus about 100,000 years." (Melosh: 1989: 129).

The meteorite's kinetic energy is distributed over both the impactor and the target rock. Some of the kinetic energy becomes internal energy during compression and can initiate shock-metamorphic effects in the rock (French, 1998). The shock wave in target rock propagates outward in a hemispherical shape with the center on average about one impactor diameter below the surface. In solid rock, the impactor will penetrate

> … no more than 1–2× its own diameter before its kinetic energy is transferred to the target rocks by shock waves generated at the interface between projectile and target … (French, 1998: 18).

When the shock wave traveling through the meteorite reaches the rear surface, it is reflected back into the now-compressed impactor as a rarefaction or release wave unloading the impactor from the high shock pressures. The contact and compression stage is considered to be over when the release wave hits the front of the impactor (French, 1998). After the release wave reaches the leading edge of the impactor and completely unloads it,

> … the projectile itself plays no further role in the formation of the impact crater, and the

> actual excavation of the crater is carried out by the shock waves expanding through the target rocks … (French: 1998: 19).

At this point, the remaining energy, around 90% of the total energy of the impactor, is thus transferred to the target (Melosh, 1989). As the impactor unloads from the high pressures it may expand into the vapor phase (ibid.). In fact, if the shock pressures are sufficient for the vaporization of the meteorite, the vapor will expand out of the crater as a high-speed vapor plume (ibid.).

The onset of 'jetting', a hydrodynamic ejection of material at high velocities, occurs with the appearance of rarefaction waves (Gault et al., 1968). The jet comes from the interface of the compressed target rock and the impactor, which is the region that has been subjected to the highest pressures, and therefore the highest temperatures. The jet, therefore, includes material in a liquid state and superheated vapor.

It is during the contact and compression stage of impact that the largest shock pressures are attained and these pressures are far greater than pressures generated during volcanic or chemical explosions. The hemispherical shock wave that propagates through the target rock weakens with expansion, but

> Rock-hard substances suddenly become compressed to unusual densities. Matter acts as though it were liquid, or at least extremely plastic … Compression effects will make rock rebound like rubber … (Baldwin, 1963: 6).

A change in the physical and chemical properties of a solid induced by a shock wave is called a shock effect. Impact or shock metamorphism results in shock effects generally seen on the scale of mineral grains and represents unequivocal evidence of meteoritic impact (Stöffler and Langenhorst, 1994). Quartz is the most reliable indicator of shock metamorphism because it is an abundant, widely distributed rock-forming mineral and displays the greatest variety of well-defined permanent shock effects. The stable form of SiO_2 in rocks of Earth's upper continental crust is trigonal α-quartz which behaves differently under shock compression than in static laboratory experiments and natural tectonic environments (ibid.).

Stöffler and Langenhorst (ibid.) propose the following petrographic classifications for shocked quartz. In the low pressure regime: planar microstructures divide into planar fractures (PF), planar deformation features (PDF) which are subdivided into non-decorated PDFs and decorated PDFs, and mosaicism, which is a highly-irregular mottled optical extinction pattern. PFs appear in parallel sets of open fissures and spacing per grain for PFs is greater than 15 μm, typically more than 20 μm. Fractures are evidence of very weakly-shocked quartz and should not be considered as diagnostic shock effects. Having said that, sets of multiple PFs *are* the product of impact-generated shock waves. Natural quartz from non-impact settings does not generally show PFs, or cleavage, and this rarity —or complete absence—of cleavage in natural quartz from non-impact settings indicates that PFs, when intensely developed in multiple sets, can be used as indicators of shock metamorphism and meteorite impact (French and Koeberl, 2010; French et al., 2004). This is especially important for the study of structures showing no other evidence of shock metamorphism, such as the Rock Elm Structure in Wisconsin.

PDFs occur as multiple sets of parallel, planar optical discontinuities, which are in fact amorphous lamellae, with spacing that ranges from 2 to 10 μm. With increasing shock intensity, PDFs become more closely spaced. Another type of PDF consists of thin multiple lamellae of Brazil twins (ibid.). Stöffler and Langenhorst (1994: 168) state that

> It is absolutely mandatory that any claim to have observed shock-induced PDFs in quartz at least must provide data on the crystallographic orientation and the (clearly defined) frequency of PDFs based on stereographic projections of universal or spindle stage data.

In the high pressure regime, shock effects include: diaplectic quartz glass (shock-amorphized quartz), the high-pressure polymorphs coesite and stishovite, silica glass (lechatelierite) and the condensation products of shocked vaporized quartz (Stöffler and Langenhorst, 1994). Stishovite is formed at lower pressures than coesite because stishovite is formed during shock compression and coesite crystallizes during pressure release. French and Koeberl (2010) note that even though post-stishovite phases have recently been reported from deep-seated mantle rocks under ultra-high pressure, stishovite remains an excellent indicator of impact when found in sediments or upper crustal rocks. Table 1 lists shock pressure and effects during impact.

4.3 Excavation and Ejection

The high pressures of the contact and compression stage decline rapidly during the excavation stage as the shock wave expands and weakens due to being spread over a larger volume of target material. Excavation begins and the crater cavity opens, forming the transient crater as ejecta begin to move upward and outward (French, 1998). The shock pressures are greatest directly below the impact site, but do not vary much over the expanding hemispherical shell (Melosh, 1989). As pressure increases, yield strength for intact target rock increases, however the strength of rock, both intact and fragmented, decreases

Table 1: Shock pressures and their effects (after French, 1998: 33).

Approximate Shock Pressure (GPa)	Estimated Postshock Temperature (°C)*	Effects
2–6	<100	Rock fracturing; breccia formation
		Shatter cones
5–7	100	Mineral fracturing: (0001) and $\{10\bar{1}1\}$ in quartz
8–10	100	Basal Brazil twins (0001)
10	100*	
		Quartz with PDFs $\{10\bar{1}3\}$
12–15	150	Quartz → stishovite
13	150	Graphite → cubic diamond
20	170*	
		Quartz with PDFs $\{10\bar{1}2\}$, etc. Quartz, feldspar with reduced refractive indexes, lowered birefringence
>30	275	Quartz → coesite
35	300	
		Diaplectic quartz, feldspar glasses
45	900	Normal (melted) feldspar glass (vesiculated)
60	>1500	Rock glasses, crystallized melt rocks (quenched from liquids)
80–100	>2500	Rock glasses (condensed from vapor)

* For dense nonporous rocks. For porous rocks (e.g., sandstones), postshock temperatures = 700°C (P = 10 GPa) and 1560°C (P = 20 GPa). Data from *Stöffler* (1984), Table 3; *Melosh* (1989), Table 3.2; *Stöffler and Langenhorst* (1994), Table 8, p. 175.

with increasing temperature (Collins et al., 2004). Target rocks are heterogeneous and so respond non-uniformly to shock and deformation during the cratering process, resulting in a range of deformation features displayed in any particular zone (ibid.).

The shock wave continues to expand throughout excavation degrading into a stress wave and then into an elastic wave. The rate of decline of the strength of the shock wave determines the amount of vaporized or melted target rock, and

> The mass of melt is roughly ten times larger than the mass of vapor. This general relation is a simple geometrical consequence of the rate of decline of pressure with radius. (Melosh, 1989: 64).

Energy available to drive the expanding shock decreases as it spreads and is consumed in heating, melting and vaporizing material. An excavation flow begins after the shock wave has passed the now-shocked target materials, and the first ejecta to leave an impact crater is the vaporized meteorite and target material expanding out of the growing crater.

> Impact velocities must exceed about 10 km/second for significant amounts of vaporization in either silicate or water ice impactors or targets. (Melosh, 1989: 68).

A gas plume will move faster than the classic ejecta and enclose the expanding crater in an atmosphere of vaporized meteorite and target rock (ibid.). Although jetting initiates mass ejection from the forming crater, most of the ejected material is removed later under lower stress conditions and with modest ejection velocities (Gault et al., 1968). The ejected material moves up and out from the growing crater in a steady flow that develops into an inverted, conical-shaped debris curtain above the target surface.

Fractured rock is weaker than intact rock and porous rock, when compressed, initially compacts with no associated rise in strength (Collins et al., 2004). Porous target material is not an effective translator of shock waves, consequently, the shock exists only in the vicinity of the projectile (Kadono, 1999). Porous target material contains a solid component and a void-space component. Wünnemann et al. (2006) investigated the effect of porosity and internal friction on transient crater formation through numerical

modeling and found that both play a role in limiting crater growth, especially in cases where gravity is much less than the Earth's gravity. Their porous-compaction, ε-alpha, model accounts for the collapse of pore space by assuming the compaction function depends, not on pressure, but on volumetric strain. The crushing of a large volume fraction of void space in porous targets absorbs shock waves and results in higher post-shock temperatures than impacts into non-porous targets. More energy is required to produce impact craters of the same size in porous targets than in non-porous targets.

The volume fraction of void space in target material, or porosity, ϕ, for a target of total volume V_T, with solid component volume V_S and pore space volume V_V, is given by:

$$\phi = (V_T - V_S)/V_T = V_V/V_T \quad (16)$$

If ϕ, = 0, then there is no void space in the target, whereas $\phi = 1$ implies no solid component. Therefore, if ρ_T is the bulk density of porous rock and ρ_S is its solid component density, then

$$\rho_T = \rho_S(1 - \phi) \quad (17)$$

Changes in the bulk density of porous target material are due to both the compaction of pore space and compression of the solid component. In an idealized example, all pore space is crushed out before any compression of the solid component takes place.

The amount of resistance to volume change and amount of irreversible work done in porous versus non-porous material is different because it is easier to compact a porous material than to compress a non-porous sample of the same material. The ε-alpha model is a way of describing the crushing of pore space as a function of compressive stress (Wünnemann et al., 2006). The P-alpha model provides a simple way of computing the compaction of void space in porous material from applied pressure, P. In this model, a distension parameter, α, is given by:

$$\alpha = 1/(1 - \phi) = V_T/V_S = \rho_S/\rho_T \quad (18)$$

So, for some amount of porosity, $0 < \phi < 1$, the model indicates $\alpha > 1$ (ibid.).

The greater amount of irreversible work performed on porous target material raises its internal energy to a higher level as compared to non-porous material. In non-porous target material, the kinetic energy of impact results in rapid material compression giving rise to the generation and propagation of a shock wave. In porous material, most of the impact energy is utilized in the irreversible crushing of void space. Shock waves decay more rapidly in porous material due to the compaction of pore space. Therefore, a crater formed in porous material is deeper and smaller in diameter than one formed in non-porous material by the same amount of impact energy since the lower bulk density of the porous material allows for the deeper penetration of the projectile (Wünnemann et al., 2006). It is also possible that lower shock pressures in porous target material may result in less resistance due to friction. The ε-alpha model indicates that the effect of porosity is to reduce the diameter of a transient crater in porous relative to non-porous material uniformly for all projectile sizes and all gravitational accelerations. However, when internal friction is varied independently, the reduction of transient crater size becomes more significant with decreasing gravity and projectile size (ibid.).

A projectile appears as a point source when any crater-related phenomena occur far from the point of impact (Housen and Holsapple, 2011). Small craters in cohesive materials form in a 'strength regime', because it is the impactors' material strength, Y, which determines the crater size. For larger craters, gravitational forces dominate any strength, so gravity, g, determines the crater size in the 'gravity regime' (ibid.). There are various strength measures of a material including compressive, shear, tensile, and others. The effect of target properties such as strength and porosity on ejecta is not understood, nor is the effect of speed. Housen and Holsapple (ibid.) developed a point-source scaling model for ejecta mass and velocity distribution to fit data for materials distinguished by porosity. Energy is lost during compaction of pore spaces which results in a reduction of ejection speeds. For launch position, x, at which a particle with ejection velocity v crosses through the plane of the original target surface of density ρ, and a, U and δ are the impactor's radius, velocity, and mass density respectively, the ejecta velocity distribution can be described by either

$$v/U = C_1[x/a(\rho/\delta)^{\nu}]^{-1/\mu} \quad (19)$$

where C_1 is a constant determined from fits to data and the exponent μ depends on the high pressure properties of the target, or

$$v/(gR)^{1/2} = C_2(x/R)^{-1/\mu} \quad (20)$$

where R is the apparent radius of the final crater. The choice of which equation to use depends on whether the impactor properties or the crater size is known (Housen and Holsapple, 2011). Experimental results indicate that $\mu \sim 0.41$ for dry soils and $\mu \sim 0.55$ for non-porous materials such as metal, water or rock. Though it has not yet been determined, it is expected that $\mu < 0.4$ for highly porous materials.

In high-speed impacts, the impactor and part of the target rock vaporize and expand back out of the forming crater as a hot gas, while other target rocks are melted and line the crater or

accumulate in a pool at the bottom. As the hot gas expands, around 50% of it condenses into liquid droplets or solid particles while the rest may end up as free atoms and molecules in the atmosphere or in space (Melosh, 1989). Nininger discovered large quantities of 100–200 μm nickel-iron spherules surrounding the Barringer Crater in Arizona in 1946 and believed that "… they condensed from the nickel-iron projectile that produced the crater, and their abundance supports his view." (Melosh, 1989: 70). He also notes that the spherules, however, may have "… originally formed from splashes of melted, but not vaporized, nickel-iron." (ibid.).

Ejecta begins to cover the surrounding area as the excavation opens a transient crater that is many times larger than the meteorite (Melosh, 1989). Excavation is completed in seconds to minutes depending upon crater size (French, 1998). The impact-induced shock wave expands hemispherically away from the shock point reaching the surface, which is a "… plane of zero pressure …", producing a rarefaction wave

> … equal in strength but of opposite sign to the shock wave, which starts downward from the surface as soon as the shock wave arrives. (Melosh, 1989: 71).

The sum of the pressures exerted by these two waves is zero on the surface; however, the rarefaction wave propagates downward fracturing the rock as it goes, and

> Where the stresses in the tensional release wave exceed the mechanical strength of the target rocks, the release wave is accompanied by fracturing and shattering of the target rock … (French: 1998: 20).

This causes the brecciation and fracturing found in impact structures, as the target rock is usually not crushed by the shock wave. Instead,

> … the rarefaction following the shock propagation downward and outward many times the crater depth or diameter, fracturing the rock *in tension* as it goes. (Melosh, 1989: 72).

Near-surface rocks are not only shattered, but are ejected at high speed due to the wave "… reflection process which converts some of the initial shock-wave energy to kinetic energy …" (French, 1998: 20). As the shock wave passes through, it leaves the target rock behind in motion, so this zone near the surface is "… the source of an extraordinary body of ejecta." (Melosh, 1989: 73). The excavation flow is considered to be ejected when it rises above the original target surface

Debris ejected from an impact crater is deposited with the greatest thickness along the crater rim, thinning out with increasing distance from the crater. If the ejecta forms a continuous deposit, then it is referred to as an 'ejecta blanket'. Impact crater debris tends to travel together after ejection forming, as stated earlier, an ejecta curtain with the greater proportion of melt glass and highly-shocked fragments occurring higher up in the curtain (Melosh, 1989). If an ejecta curtain forms, it has the shape of an inverted cone because

> Ejecta from near the impact site travels at high speed, whereas ejecta emerging at larger distances travels at lower velocities …" (Melosh, 1989: 75).

Melosh (ibid.) notes that high-velocity ejecta are usually highly shocked, but even the lowest velocity ejecta which will form the crater rim will contain some highly-shocked impact melt (cf. French, 1998).

Crater rims are not composed only of material ejected from the crater during excavation, but also of rock that has been pushed outward and upward. Strong compressive forces press horizontally outward from the excavating crater causing rock to fracture and then be squeezed upwards. According to Baldwin (1949) the radially-outward dip of the upraised crater rim is indicative of an impact event. About half of the rim height is due to structural uplift of target rock which is greatest beneath the crest of the crater rim and then decreases with increasing distance from the point of impact, dropping off to "… zero approximately 1.3 to 1.7 crater radii (center-to-rim-crest radius) from the crater's center." (Melosh, 1989: 87). In addition, brecciated rock is emplaced into fractures and dikes beneath the crater floor and rim during the brief time of low vertical stress after target material is thrown upward but has yet to settle back on the floor and on growing rim of the crater (French, 1998). Only the top one-third of the transient crater material is ejected, and the "… rest of the crater is excavated by displacement of target material downward and outward beneath the crater rim." (Melosh, 1989: 88).

The rest of the rim height is due to the ejecta that then lands on top of this uplift. Some of the ejected debris moves at such low speed that it retains its stratigraphy and forms an "… overturned flap …" seen as an area of "… inverted rock units." (Melosh, 1989: 87). If this material collapses into the crater, however, an overturned fold may not survive the modification stage. Ejecta that land beyond the crater rim mix into jumbled breccia that includes material from the target surface.

According to Melosh (1989: 88), crater rim height, h, for uncollapsed simple craters where D is the crater's rim-to-rim diameter, is given by

$$h = 0.036D \quad (21)$$

This formula was derived from measurements "… of many lunar, terrestrial, explosion, and lab-

oratory impact craters." (ibid.). For larger transient craters that experience a sub-sequent collapse as the overturned flap and rim crest slide down into the crater, the equation's coefficient and power of D varies depending on the surface material and gravity. According to Melosh (ibid.), for a lunar crater with a dia-meter of over 15 km, this equation takes the form

$$h = 0.236 D^{0.399} \quad (22)$$

Ejecta deposits consist of broken rock fragments, called clasts, mixed with glass. Though small rock fragments dominate the ejecta, clast size can reach many meters in diameter; in fact, the largest fragments that are ejected may form secondary craters. The larger impact craters can be accompanied by one or even more secondary craters that form clusters or lines. Secondary craters usually have steeper slopes in the direction of the primary crater becoming more circular with increasing distance from the primary. Secondary crater clusters also become more widely dispersed with increasing distance from the primary (Melosh, 1989). Clast size also decreases with increasing distance from the crater, "… an expectation that has been quantitatively verified in numerous small-scale impact experiments …" and at the Barringer Crater in Arizona (Melosh, 1989: 91). According to Baldwin (1963: 69), there is "… always a radial distribution of both meteoritic matter and crustal rock scattered over perhaps ten times the radius of the crater proper."

Crater depth is determined by the resistance of the underlying target material, but, the crater will still continue to grow in diameter after its maximum depth has been reached (Melosh, 1989). The result is a crater that is wider than it is deep. According to Melosh (ibid.), the time, T_d, required for this maximum depth, H, to be reached is

$$T_d \approx (2H/g)^{1/2} \quad (23)$$

This is basically the equation for free fall of an object falling from a height, H, with an initial velocity of zero, and with an acceleration due to gravity, g. Melosh (ibid.) also states that the time, T_f, for the transient crater with final diameter, D, to be completed is

$$T_f \approx (2D/g)^{1/2} \quad (24)$$

French (1998: 20) notes that

> The excavation stage, although longer than the contact/compression stage, is still brief by geological standards …

Depending on the transient crater size, the entire excavation process takes only a few seconds for a simple crater to less than two minutes for a transient crater that is 200 kilometers in diameter (ibid.). Gault et al. (1968) suggest that formation times for large planetary cratering events scale directly with the square root of the crater dimensions, which would indicate that the Barringer Meteor Crater formed in around 10 seconds.

The diameter of the modified final crater is rarely the same as the diameter of the transient crater that forms during the excavation stage. The collapse of the transient crater due to gravity

> … may enlarge this diameter by roughly 20 percent for small, bowl-shaped simple craters or by as much as 30 to 70 percent for the larger, more thoroughly collapsed complex craters. (Melosh, 1989: 112).

Figure 8 shows a transient crater and the final modified simple crater it would form according to Melosh (1989). After the initial modification is complete, "… the diameter of the final crater is many times larger (typically 20–30×) than the diameter of the projectile itself …" (French, 1998: 20).

4.4 Crater Modification

The excavation/ejection stage ends as soon as the transient crater has reached its maximum size (French, 1998: 23). The final stage of impact crater formation involves modification due to gravity and the elastic rebound of compressed rock layers. Masaitis (2005) points out that later modification should be divided into early and late stage modification since gravitational adjustment, viscous relaxation and doming, cooling, solidification, and compaction of the hot disturbed bed rock, fallback, and material ejected from the crater may continue for thousands of years.

After the transient crater has formed by excavation and the ejecta has been launched, the debris momentarily halts and then begins to move downward. In simple craters, this motion involv-

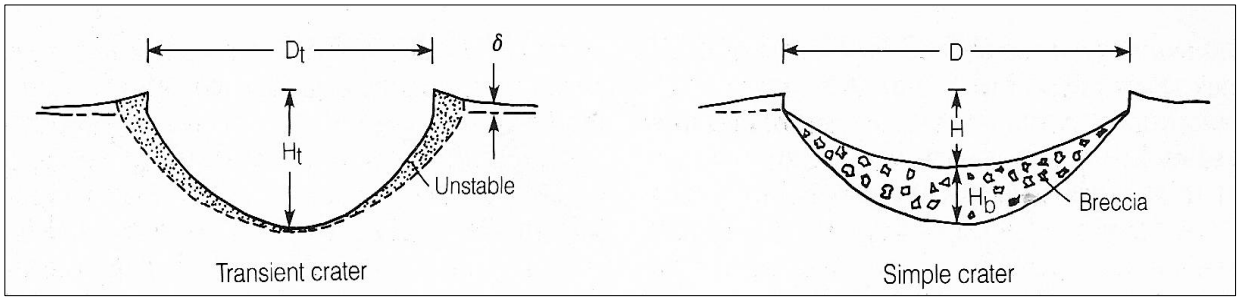

Figure 8: Diagrams showing a transient crater and the resulting simple crater (after Melosh, 1989: 129).

es fallback ejecta and debris sliding down the transient crater walls resulting in "... a bowl-shaped depression, partially filled with complex breccias and bodies of impact melt ..." (French, 1998: 20). Modified simple craters are rimmed, bowl-shaped pits that are not very different from the transient craters that formed them (French, 1998). Figure 8 shows the difference between the transient and final simple crater, the primary difference between the two being the breccia lens that covers the floor of a modified simple crater. The breccia lens consists of broken rock mixed with shocked fragments and impact melt that slides back into the crater along with part of the inner rim. The slope of the crater walls gradually decreases in the direction of the crater's center until the floor becomes flat. The thickness of the breccia lens is about half of the rim top-to-floor depth (ibid.). The final simple crater size "... is only slightly larger in diameter than the transient crater but is significantly shallower." (Melosh, 1989: 129).

In matching observational data to model predictions, Collins et al. (2005) found a first order approximation of the final rim-to-rim diameter, D_{fr}, for a simple crater in relation to the transient crater diameter, D_{tc}, measured at the pre-impact surface, is given by:

$$D_{fr} \approx 1.25 D_{tc} \quad (25)$$

For a 'fresh' complex crater measured from rim crest to rim crest, where D_c is the diameter at which the transition from a simple to a complex crater occurs, that is 3.2 km on Earth (ibid.):

$$D_{fr} \approx 1.17 D_{tc}^{1.13} / D_c^{0.13} \quad (26)$$

Pilkington and Grieve (1992) use known morphometrical scaling relationships to develop models relating impact crater diameter, D, and the effect of gravity. The true impact crater floor, marked by the base of the allochthonous breccia lens, may be filled with post-impact sediments. For this apparent crater depth, d_a, and true crater depth, d_t, (both in km) of simple craters the following empirical relationships, independent of target lithology, have been determined:

$$d_a = 0.13 D^{1.06} \quad (27)$$

$$d_t = 0.28 D^{1.02} \quad (28)$$

For complex craters formed in sedimentary lithologies

$$d_a = 0.12 D^{0.3} \quad (29)$$

$$d_t = 0.20 D^{0.4} \quad (30)$$

and for complex craters formed in crystalline lithologies

$$d_a = 0.15 D^{0.4} \quad (31)$$

$$d_t = 0.52 D^{0.2} \quad (32)$$

While simple craters experience primarily the collapse of the steep crater rim, larger transient craters are completely altered in appearance upon collapse producing central peaks surrounded by a flat floor and terraced walls due to slumping. A complex crater's final depth is shallow and the width much greater than that of the transient crater preceding collapse, as shown in Figure 9. However, this diagram is an over-simplification since it does not show the terraced walls and central uplift that are typical of a complex crater (see Figure 10). Terrestrial complex craters have depths >0.5 km, but their central peaks are seldom higher than the crater rim and are usually closer in height to the elevation of the unaltered area surrounding the crater (Melosh, 1989). Central peak diameter is 0.22 $\pm$ 0.03 of the crater's diameter and is "… apparently independent of the planet on which the crater forms." (Melosh, 1989: 132). This statement includes not only the Earth,

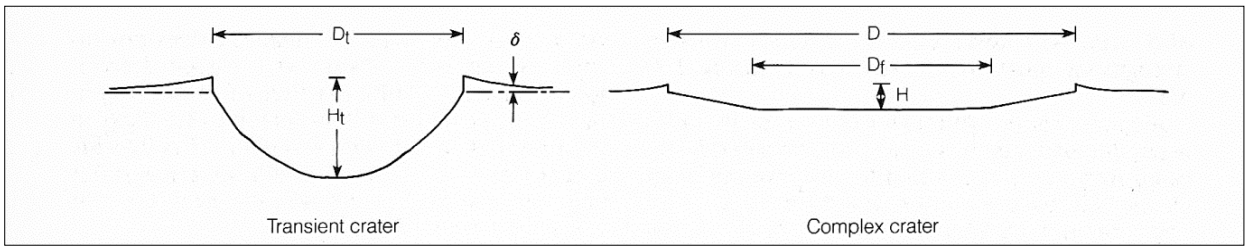

Figure 9: These diagrams show the final crater diameter, D, of a complex crater compared to the smaller diameter, D_t, of the transient crater, and the transient crater's depth, H_t, which is greater than the complex crater depth, H (after Melosh, 1989: 144).

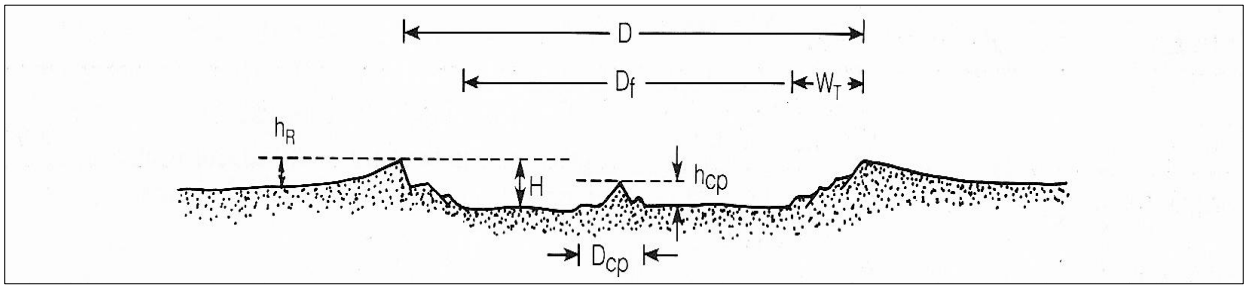

Figure 10: The final form of a complex crater, including the central uplift and terraced walls. Here W_t is the width of the terraced zone, D_{cp} is the diameter of the central uplift and h_{cp} is its height (after Melosh, 1989: 132).

Mercury, and Mars, but also our Moon and perhaps Ganymede and Callisto (ibid.). For larger craters, the diameter of an inner peak ring is about half the crater rim diameter or $D_{PR} = (½)D_F$ (ibid.).

The sudden onset of complex crater collapse indicates that a definite strength threshold has been exceeded beneath craters larger than a critical size (Melosh, 1989). This strength threshold (ST), in kg/ms^2, can be estimated by dividing the negative buoyancy force associated with the crater cavity by the area of a hemisphere enclosing the crater, that is:

$$ST = (\pi/8)\rho g H D^2/(\pi/2)D^2 = \rho g H/4 \quad (33)$$

for rim-to-rim diameter D, rim-to-floor depth H, and density ρ, where g is the acceleration due to gravity. Slip-line analysis applied to the collapse of impact craters gives an accurate description of their collapse (Melosh, 1989). Materials fail when the shear strength exceeds a defined yield stress called cohesion, c. In terms of the transient crater diameter D_t and height H_t, parabolic craters are stable until the parameter $\rho g H_t/c > 5$. Slope failure, that is when a rim segment slides into the crater producing a terrace, occurs for $10 > \rho g H_t/c > 5$. If $\rho g H_t/c > 15$, then "… the floor beneath the center of the crater rises almost vertically upward as the rim slumps downward …" (ibid.). For a transient crater diameter $D_t = 0.27H_t$:

$$0 \leq D_t \leq 13.5\ c/\rho g, \text{ stable} \quad (34)$$

$$13.5 \leq D_t < 27\ c/\rho g, \text{ slope failure} \quad (35)$$

$$27 \leq D_t < 40\ c/\rho g, \text{ floor failure} \quad (36)$$

Final depth of a complex crater, H, is independent of the initial crater's diameter and is found by:

$$H \sim 5c/\rho g \sim H_{threshold} \quad (37)$$

Roddy and Davis (1977: 744) determined that *in situ* shatter cones "… point in the direction of the shock wave source with their axes normal to direction of shock wave propagation." French (1998) agrees that the orientations of shatter cones axes found in rock surrounding terrestrial complex craters point to the location of the source of the shock wave that formed them. The mapping of shatter cones often show them pointing upward or even outward in the crater's central region, and

> The simplest explanation of this observation is that the rock units were uplifted and tilted away from the crater center following the passage of the shock wave … (Melosh, 1989: 140).

If the original crater shape is reconstructed from the orientation of shatter cones, then the crater is found to originally have a deep bowl shape with a depth/diameter ratio about equal to that of the transient crater (ibid.). Terrestrial crater structural studies indicate that modification from the transient to the complex crater involves the extensive and general collapse of the initially-deep transient crater, and is achieved by uplift of target rock under the crater center and by rock nearer the crater's rim slumping downwards and inwards (ibid.)

The central uplifts found in terrestrial complex craters are composed of fractured and deformed rock that was originally under the transient crater. This rock has been uplifted a distance that is comparable to the transient crater depth and is not a breccia mix like that found in simple craters. Melosh (1989) also notes that the central stratigraphic uplift, SU, referred to as the height, h, in this equation, can be related to the final diameter of the crater, D, by

$$h_{SU} = 0.06D^{1.1} \quad (38)$$

The stratigraphic uplift is about half the depth of the transient crater (ibid.). From a study of 24 complex terrestrial impact structures, Grieve and Pilkington (1996) suggest that structural uplift (<u>StU</u>) where D is the rim diameter of the impact structure is given by:

$$StU = 0.086D^{1.03} \quad (39)$$

French (1998: 25) points out "… the two equations [38 and 39] are virtually identical, and a value of $StU = 0.1D$ is a reasonable approximation to either." He also states that even in the largest structures,

> … both theoretical and field studies indicate that central uplifts form in only a few minutes, almost instantaneously by geological standards (ibid.).

According to Baldwin (1949: 149), during the contact/compression stage of an impact event, a great deal of momentum is transferred to the compressed target rock which then rebounds during the initial modification stage to become fixed as a structural dome. When the tremendously-hot and compressed plug of rock and meteorite explodes violently, it results in "… a series of concentric waves …" moving outward in all directions which will result in ring synclines and anticlines in rock at the site of impact (Baldwin, 1949: 99). Anticlines fold downwards on both sides and synclines fold upwards on both sides from a median line of rock strata. The largest structures have more than one ring surrounding the impact site and are referred to as multi-ring basins (French, 1998).

Central peaks form in the modification stage of impact according to Milam and Deane (2005), as follows. During the contact/compression stage, deformation causes weakening of the rock which allows for the movement of large blocks of rock in the central area of the impact crater. The target rock typically is fractured, faulted and shows signs of melting and shock deformation.

When the resulting pressure is released, a rebound of target material occurs allowing large blocks of rock to move upwards. The "… major faults are likely responsible and represent the final stages of central uplift formation." (Milam and Deane, 2005: 2). This rock then becomes fixed structurally as it is damped by tension fractures. They also note that an uplift is often surrounded by a ring syncline and possibly an anticline. If the central peak is over-steepened or weak, then it may collapse forming a series of structural ring structures in sedimentary target rock since it is much less resistant to horizontal movement than crystalline rock (Ferriere et al., 2011). Luizi is a confirmed impact structure in the Democratic Republic of Congo that displays just such structural rings: a ~2 km wide central ring surrounding a central depression along with a ~5.2 km intermediate ring which is in turn surrounded by an annular depression and an elevated rim some 17 km in diameter.

French (1998) agrees that it is during the modification stage after the excavation and ejection of target rock that the central uplift will rise. Once a meteorite impacts a solid surface and blasts out a large impact crater, the underlying rock is compressed downwards and outwards and then rebounds upwards and inwards. The rock cannot fall back to its original position since that original space is now filled in by rock that has moved in from the sides. French (1998: 24) gives the following description:

> A simple model of the formation of a complex crater and its central uplift is presented by the familiar slow-motion movies of a drop of liquid hitting a liquid surface … There is the same initial cavity formation, the same outward and downward ejection of target material, the same upward rebound of the central cavity floor, and the same collapse of the periphery back into the cavity.

During impact,

> Rock-hard substances suddenly become compressed to unusual densities. Matter acts as though it were liquid, or at least extremely plastic … Compression effects will make rock rebound like rubber … (Baldwin, 1963: 6).

As stated, Baldwin (1963:107) suggests that rebound is responsible for central uplifts. In this scenario, rocks below the crater have been strongly compressed by the impact force and then spring back when the stress is relieved, causing the crater floor to move upward forming a structural dome. Most structures exhibit this shock-wave rebound pattern with a central dome when enough time has passed for erosion to expose the basement structure, and in the central regions a jumble of shattered and brecciated rock is found. The impact structures we study today, though, may not give a true indication of the original appearance of complex craters since it is only the basement structure of an impact crater that is visible after extensive erosion, and

> The fact that all the highly eroded impact structures show a central rebound dome does not imply that all the original craters exhibited central peaks. (Baldwin, 1963: 108).

If enough fallback breccias filled the crater, the peaks may have not have been of a sufficient height to extend through the breccias.

Melosh (1989: 141) makes an interesting observation:

> This process has no obvious dependence on gravity or crater size, and so probably cannot explain the central peaks of complex craters …

although it may explain central peak formation in impact craters where the impactor made only a very shallow penetration of the target rock. Melosh instead believes that geological and morphological evidence supports complex crater development from a bowl-shaped transient crater, and that it is gravity driven (ibid.). Melosh (1989: 142) gives the following equation for time, T, required for the rise of the central peak:

$$T \leq (D/g)^{½} \tag{40}$$

and he believes that the crater floor uplift starts before the rim is fully formed. This would indicate that the complete parabolic transient crater never completely forms, since the uplift begins as soon as the final transient depth is reached and before the rim is completed.

Melosh (ibid.) also notes that breccia lenses are not found in the centers of complex craters, indicating a collapse that is so rapid that there is not enough time for debris to slide down the transient crater walls. Instead, breccia in complex craters fills a ring depression located between the crater's rim and central uplift. Complex crater floors are covered with breccias and melt rock that lie in the same stratigraphic sequence that lined the transient cavity (ibid).

Melosh (1989) believes that the terraces surrounding the crater floor form quickly, before the impact melt has time to solidify. He points out that complex crater

> … terraces fade smoothly into the solidified impact melt covering the crater floor without any sign of disruption by movement after the melt solidified … (Melosh, 1989: 142).

Crater terraces are widest near the rim and tend to narrow toward the central region.

Melosh (1989: 143) points out that rock debris motion within a forming crater is apparently "… fluidlike, involving rapid uplift of a central peak, analogous to the central jet that forms when a cavity in water collapses …", which is in agree-

ment with Baldwin (1963) and French (1998), indicating that if central peaks do form by a hydrodynamic mechanism then the rock beneath the crater must behave as a fluid during uplift. Unlike the flow in a fluid, however, the flow in a forming crater is 'frozen' at some point depending upon the crater's size and the viscosity of this fluid, and "The central peak is, in effect, a damped harmonic oscillator …" (Melosh, 1989: 147).

One early idea that was proposed for the fluid-like behavior of rock debris in impact craters was that it was

> … fluidized by impact melt. The debris flows briefly as a melt-solid slurry until it cools and solidifies … (Melosh, 1989: 151).

Although some impact melt is found on complex crater floors, it is only rarely found in central uplifts or in the stratigraphical uplift region beneath the crater where the fluidization would be required. Melosh (1989: 154) suggests that "… crater collapse facilitated by acoustic fluidization."

Although the crater collapse process is reasonably well understood for the smaller, simple craters, the collapse of complex impact craters is still a poorly-understood process that has a profound influence on the final morphology of the crater (Collins et al., 2004). This is due to the fact that there has not been a direct observation of complex crater collapse in recorded history, and the limitations of small-scale laboratory experiments. Since crater collapse is gravitationally driven, small-scale experiments cannot be extrapolated meaningfully to the scale of complex craters. There is evidence that natural rock is weaker on scales of tens to hundreds of meters with respect to laboratory strength measurements of centimeter-scale rock samples. The best avenues for studying complex crater collapse are computer simulations and observational analysis of impact structures, however, damage due to impact must be carefully interpreted when numerical modeling is utilized (ibid.).

Shatter cones have been considered proof of impact for decades; however, their formation is still not well understood. Numerical simulations of impact using the hydrocode SALE 2D, enhanced by the Grady-Kipp-Melosh fragmentation model, suggest that shatter cones are initiated by heterogeneities in the target rock (Baratoux and Melosh, 2003). With pressures of 3-6 GPa, if the shock wave travels faster in target rock than in the heterogeneity by a minimum factor of around 2 and the dimensions of the heterogeneity are comparable to the width of the shock wave, both of which are smaller than the resulting shatter cone, then according to the model a shatter cone will form. Based on this model, the apical angles of shatter cones seem to depend on the properties of the heterogeneity and the decay time of the shock wave. The angle of the shatter cone, θ, may be found by:

$$\theta(t) = 2 \arccos (1-\beta\tau/\delta t) \quad (41)$$

where τ is the rise time and $\beta\tau$ is the decay time of the stress wave, and δt is the time elapsed since contact between the shock front and the heterogeneity (ibid). The authors suggest that this model should be validated by new measurements of the shapes, sizes and distribution of shatter cones in various impact sites.

Collins et al. (2005) have developed a Web-based program that calculates regional environmental devastation of a terrestrial impact requiring only six descriptors: meteoroid diameter and density, meteoroid velocity before atmospheric entry, impact angle, the distance from impact at which the environmental effects are to be calculated, and whether the target is sedimentary rock, crystalline rock, or a water layer above rock. The most far-reaching environmental consequence is seismic shaking since ejecta deposit thickness and air-blast pressure decay more rapidly with distance than does seismic ground motion. The most devastating effect is thermal radiation close to the impact site. Melosh (1989: 212) gives the radius, R (in meters), of a vapor cloud formed in a high velocity impact as:

$$R = [(3V_i/2\pi)(P_i/P_a)^{1/\gamma}]^{1/3} \quad (42)$$

where V_i and P_i are the initial pressure and volume of the gas, P_a is the pressure of the ambient atmosphere, and γ is the ratio of specific heats of the gas. If the energy, E_a (in joules), deposited in the atmosphere by the vapor plume is known, then (ibid.)

$$R = 0.009E_a^{1/3} \quad (43)$$

4.5 The Howell Structure as a Meteorite Impact Scar

Back in 1937, Boon and Albritton pointed out that long after a meteorite crater and its associated ejecta and meteorite fragments have been removed by erosion and weathering, an impact structure, or 'meteorite scar', may persist in the geologic record. Figure 11 is a cross-section through a hypothetical meteorite impact crater according to Boon and Albritton, but the actual appearance of the crater remnant will depend on the extent to which it has been eroded. It is

> … only in the initial stage (along the profile AA) that the crater clearly reflects its origin in the rim of ejected material, silica glass, and meteorite fragments distributed around it. The scar will become inconspicuous when the country is denuded to level BB. When the area is down to the level CC the underlying structures begin to appear, and when the depth DD is reached the central uplift and ring folds become apparent. Should erosion proceed to depths below those affected by the

> meteoritic disturbance, the scar would be obliterated.. (Boon and Albritton, 1937: 56).

Given the age of the surrounding lithostratigraphic units, the extent of erosion during the ensuing years and the lack of any surface evidence of a central uplift, the Howell Structure is represented by the DD transect in Figure 11.

5 CRYPTO-CONTROVERSIES

Fossil meteorite craters display certain characteristic features, such as circular limits of deformation, and faults and joint sets that are within a crater's area of deformation and to some lesser extent outside of the area of deformation, that usually "… demonstrate a striking radial symmetry …" (Woodruff, 1968: 19). Dietz (1960: 1781) points out, however, that

> … the formation of a chaotic, circular structure, extensive brecciation, and intense shattering are all suggestive of meteorite impact but are hardly definitive.

In addition, an actual impact structure may not be easily recognized due to subsequent geological processes:

> The actual crater morphology of such features may have been destroyed until only the "roots" are exposed, as is the case at Wells Creek, or the crater floor may have been preserved (but at the same time kept from view) by crater filling as is seen at Flynn Creek. (Woodruff, 1968: 18).

Cryptoexplosive structures have been attributed to various mechanisms, including salt-doming. Born and Wilson (1939) believe that the Wells Creek, Flynn Creek and Howell sites were not formed as a result of salt-doming:

> In a region where salt beds are unknown, either at the surface or in subsurface drilling records, salt domes could hardly be expected to occur. Furthermore, salt-doming is not believed to be sufficiently explosive to blow out a crater 2 miles [3.2 km] in diameter and 300 feet [90 meters] deep, as in the Flynn Creek disturbance. (Born and Wilson, 1939: 379).

Woodruff (1968: 17) agrees, stating that

> Although there are some who would attribute the deformation to such geologic processes as salt dome collapse, these ideas have been discredited because of gross lack of evidence …

Woodruff (1968: 17–18) then addresses the remaining possibilities for the origin of Howell and similar sites:

> Generally, there are two schools of thought about the origins of the roughly circular, highly deformed areas as seen at Howell, Wells Creek Basin, Flynn Creek, and many others … One school attributes the origin to meteor impact, the other attributes the origin to "cryptovolcanic explosions" yielding a breccia pipe from depth.
>
> The meteoritic hypothesis brings to bear on the subject the concept of shock metamorphism … Shock processes, unlike classical metamorphic processes, occur over time intervals of "from a few microseconds to a fraction of a minute."
>
> The problem in dealing with such areas of deformation in the field is to define characteristics that are unique to the shock processes and characteristics unique to "cryptovolcanic

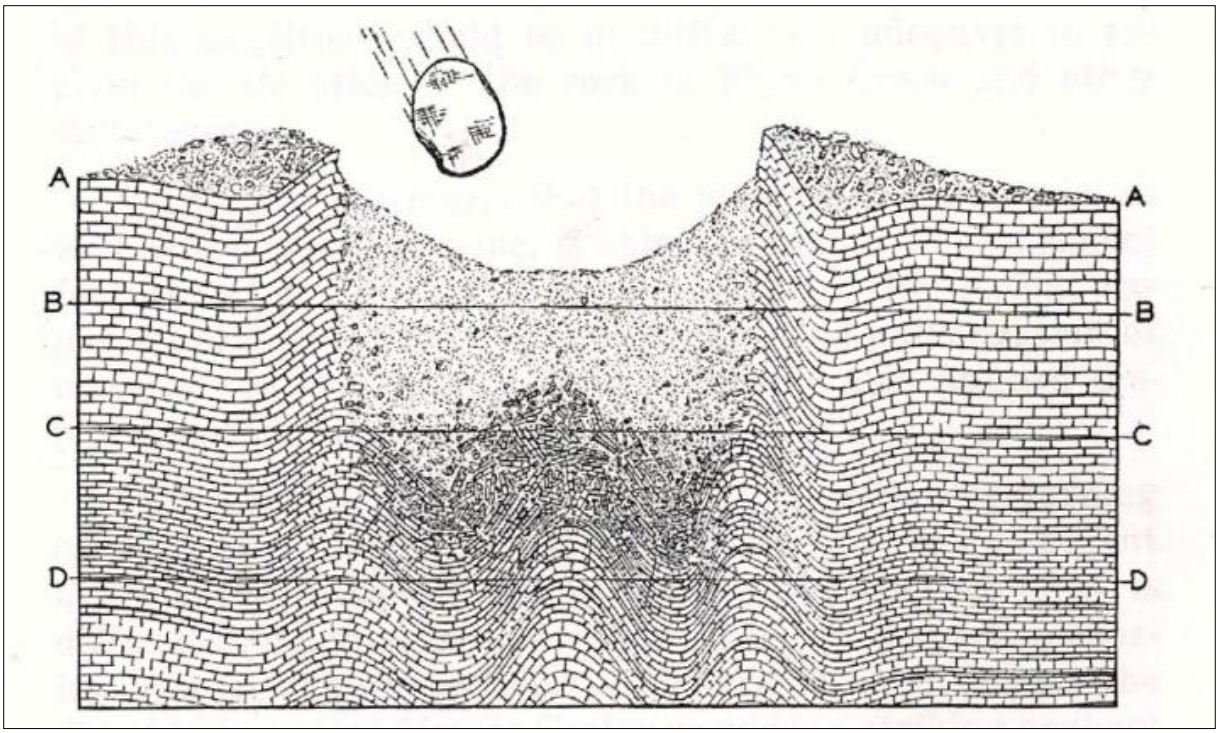

Figure 11: A section through a typical explosive impact crater caused by a meteorite (after Boon and Albritton, 1937: 57).

> processes." In finding one or another of the features, the structure can then be classified as either of "terrestrial" or of "shock" origin. In reality, however, the differentiation of the structure into the two types is not so clear cut. What a geologist has to deal with usually are only remnants of structural features that have been exposed to geologic processes for millions of years. All one finds are either greatly eroded structural features, or features that have been buried during subsequent ages. After such processes as erosion, deposition of new sediments, and possibly other structural events have sufficiently clouded the issue, the differences between features caused by shock processes in a fraction of a second, and slower formed tectonic features (and even salt dome collapse structures) become insignificant, and similar features in common become striking.

Woodruff (1968: 18) believes that

> The process that affected the Howell area in particular and certain other structures in general, were believed sufficiently explosive to have formed a crater.

Born and Wilson (1939: 379) agree, stating that they believe

> … the Flynn Creek and Howell craters, with associated injected breccias and powdered limestone, require extremely violent explosive action.

They also point out that any explanation for the structural features found at the Howell site must be able to account for the following:

> (1) a circular mass of jumbled and brecciated limestone, part of which has been uplifted approximately 100 feet [30 meters] relative to surrounding strata; (2) the shattering of Black River and Trenton limestone into blocks and the irregular jostling of these blocks; (3) the pulverizing of much of the limestone into "rock flour"; (4) the unusual ability of breccia and rock powder to force their way into fractures; and (5) the formation of a crater 1 mile [1.6 km] in diameter and more than 100 feet [30 meters] in depth, centered over the brecciated area. (Born and Wilson, 1939: 378).

Born and Wilson (ibid.) note that the above features are characteristic of the cryprovolcanic structures described by Bucher (1936), "… as well as the Wells Creek basin and the Flynn Creek disturbances in Tennessee …" which are both confirmed sites of meteorite impact. Born and Wilson (1939: 380) attribute the Howell Structure to

> An explosion, blowing out a crater at least 100 feet [30 meters] in depth and 1 mile [1.6 km] in diameter, and piling up limestone debris around the crater …

and they conclude:

> The writers recognize difficulties in both the cryptovolcanic and the meteoritic hypotheses and for the time being, prefer to maintain as neutral a position as possible until more data are found. Unfortunately, the Howell disturbance does not present new features that will aid greatly in determining the origin of this group of structures. (ibid.).

They also note that the possibility of a

> … post-Fernvale and pre-Chattanooga renewal of the same localized force that formed the pre-Fernvale crater would support the cryptovolcanic hypothesis … (ibid.).

Woodruff (1968: 19) also addresses the possible cryptovolcanic genesis of structures such as Howell:

> The presence of volcanic material may seem to be strong evidence toward the hypothesis. However, the presence of volcanic matter associated with the "fossil crater" is not unequivocal for that origin. Shock processes might well cause extensive fracturing at depth, and thus cause a drastic change in pressure which in turn might affect the geothermal gradient. Partial melting might occur with ready-made fissures for access to the surface.

Woodruff (1968: 29) also states:

> From the other evidence available – depth of deformation, roughly circular plan view and radial symmetry of geologic features, most of the Howell breccia has been categorized by this writer as being of shock type.

This would indicate that Howell is "… the ancient eroded equivalent of a meteor impact crater …" which then requires an in-depth investigation of the breccias found at Howell for confirmation (ibid.).

6 HOWELL BRECCIAS

Breccia is rock that consists of angular fragments in a fine-grained matrix. Though commonly found in confirmed impact structures, breccia is not unique to impact sites:

> Breccia may be formed by diverse processes, ranging from explosions of nuclear magnitude to collapse of solution cavities and including diagenetic breccias, fault breccias and volcanic breccias … (Woodruff, 1968: 29).

Woodruff (ibid.) points out that the end result of all of these processes is the same, but examination of the breccias themsleves does not usually give any indication of their geological origin so other evidence must be examined and considered in order to determine the genesis.

Woodruff (1968: 19) makes the interesting comment that when it comes to impact structures, breccia

> … which is so prevalent that it is used (or misused) as indication of what rocks have been affected by the structural event and which rocks have not … [is utilized in determining] the limits of deformation both laterally and vertically.

He continues, noting that

> … the extreme case of deformation is seen as breccia, and it is this criterion that has heretofore been the determining factor as to the limits of the structural features … (Woodruff, 1968: 22).

Woodruff (1968: 23) considers "… the best criterion for deformation at Howell is the presence of breccia." Meanwhile, the actual breccias found at the Howell site provide the best way of determining which rock units were deformed by an explosive event and which rock units were not involved. Woodruff (ibid.) also notes that

> … the discovery of breccia in upper-most Ordovician, Silurian, and maybe in Devonian units is of importance … mainly because of their addition to the knowledge of the extent and age of the deformation …

Born and Wilson (1939: 373) found that breccias composed of angular fragments of limestone occupied a circular area 1 mile [1.6 km] in diameter and centering around Howell, and that

> The fragments range in size from shot up to large blocks many feet in dimension and occur in a matrix of powdered limestone. Much of this breccia consists of small, angular to subangular fragments the size of walnuts. Within this type of shatter breccia occur large angular blocks of limestone that may or may not be brecciated. Many of these blocks of limestone are cut by dikelike stringers, or veins, of injected powder breccias, which suggest forceful intrusion along fractures while the injected material had a "mushlike" consistency.

However, Woodruff points out that even if Howell is an impact structure, not all of the breccia is necessarily due to shock processes. The various breccia types may be

> … a primary feature, pre-deformation, or as a secondary feature, post-deformation. One is very likely to find fault breccias, slump breccias, or collapse breccias associated with such a structure … (Woodruff, 1968: 29).

Woodruff then focuses his discussion on the formation of various types of breccias in events that are sufficiently catastrophic to yield craters. Breccias can be fragmented and granulated in place or form as "… fall back – particles thrown into the air by the explosion, but resettling into the crater proper …" (Woodruff, 1968: 30). He points out that crater fill could consist of a 'hodge-podge' of fall back, in-wash or crater rim material, and he believes that if any reworked rim material is still present at the Howell site, then it will be found only on the high ridges in the eastern section of the structure.

Woodruff (1968: 31) reports that in breccia formation,

> The same stratigraphic unit may be found to react differently to the deforming forces in different areas, reflecting various "zones" of deformation …

both laterally and vertically. He points out that "Zones may be seen in which bedding and other stratigraphic features are preserved with breccias injecting joints and bedding planes …" (ibid.), and he explains his interpretation of some of the breccia characteristics as follows:

> This retention of "relict" features with brecciation superimposed either concordantly or discordantly has been taken to indicate the fringes of deformation, especially at depth. In other words it would be where the deformation "dies with a whimper" and the forces are not sufficient to obliterate the pre-disturbance sedimentary features. (Woodruff, 1968: 31–32).

Woodruff describes the Howell breccias as generally being composed of angular to subangular fragments that grade in particle size from 'pea-size' up to blocks several meters across embedded in a matrix which most often has a sugary appearance that is gray-brown, but occasionally distinctly pink in color. He also points out that "Certain rock units may be recognized as being matrix material of certain breccias …" (ibid.). Some of the Howell breccias found by Woodruff were homogeneous, while others were mixtures of lithogies. As an example, he notes that

> … the Catheys-Leipers breccias present a hodge-podge of lithogies, in which the fragments appear to be of one rock type while the matrix appears to be another … (Woodruff, 1968: 32).

In contrast, "… the Fernvale Limestone yields a homogeneous breccia …" (ibid.).

Fossil remains were found within the brecciated rocks. A specific point of interest noted by Woodruff is that although 'fossil hash' would be expected to be preserved in breccia where fossiliferous rock units existed before the explosive event occurred, "… in at least two locations large fossils (coral heads) have been found within the breccia …" (ibid.). These coral heads are "… widely separated in stratigraphic extent …" with one sample intact within the breccia and the other with Favosites coral heads that are up to 15 cm in diameter (ibid.). Miller (1974: 22) explains that

> Corals appeared for the first time in the geologic column in Tennessee during the Ordovician time and grew in abundance in what is now the Central Basin area.

There are several different breccia types that were found and photographed by Woodruff at the Howell Structure. He describes the Howell Mega Breccia as being large blocks of rock broken apart and

> … disarranged at random orientations to one

Figure 12: A photograph of the typical Howell 'mega-breccia' matrix (after Woodruff, 1968: 34).

> another … with more 'normal' fine breccias filling the interstices between the blocks. (Woodruff, 1968: 33).

The mega-breccia blocks may themselves be brecciated. Figure 12 shows a photograph taken by Woodruff (1968: 34) at Howell of the typical 'mega-breccia' matrix he found there. Next he describes Crush Breccia or Injection Breccia by noting that "… the rocks seem to have been granulated in place without significant movement of rock material …" (ibid.). Figure 13 shows an example of the crush breccia Woodruff (1968, 35) located in Howell, which often displays relict bedding. Woodruff (1968: 36) notes that large quantities of vein injection breccia are seen in the crush-breccia, especially in creek beds, and that the veins cut across still-preserved bedding features. Figure 14 is a photograph taken by Woodruff (1968: 37) which shows a possible breccia injection vein that crosses relict bedding. Figure 15 shows what Woodruff (1968: 38) describes as a "Breccia vein showing flow pattern of fine-grained brecciated particles around larger fragments." Woodruff (1968: 33) interprets this finding to indicate that the crush-breccia rock units most likely experienced greater pressure and "… could only readjust on a small scale to the shock." In contrast,

> … the mega-breccia may generally represent a shallower zone of the deformation, and could readjust to the shock by a bulk movement of rock material … (Woodruff, 1968: 33, 36).

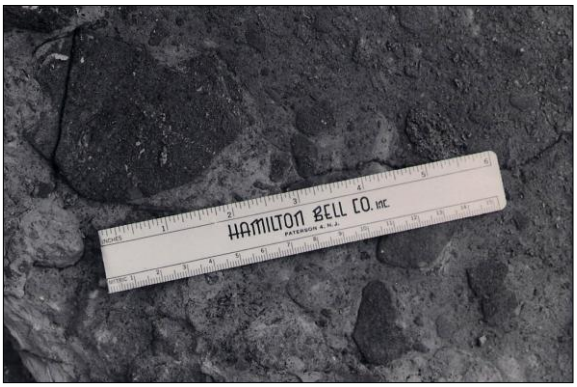

Figure 13: A photograph of the Howell 'crush breccia' (after Woodruff, 1968: 35).

The Plum Pudding Breccia Woodruff only saw in the Fernvale Limestone breccias. He states that

> … this feature was attributed to slump and crater fill … [and] the rock unit consists entirely of ferruginous limestone fragments in a matrix of the same material … (ibid.).

Figure 16 shows two photographs Woodruff (1968: 39) took of the plum-pudding breccia. The first shows it in an outcrop, and the second is a close up which shows the fragments and matrix with identical lithologies.

An unexpected finding by Woodruff involves the mix, or lack thereof, of breccias of various stratigraphic units involved in the Howell Structure:

> One would expect in dealing with an area which has been subjected to as severe a shock as meteor impact, that breccia formed would consist of a random mixture of all stratigraphic units involved. There should, it would seem, be no means of distinction between pre-deformation rock units. Certainly contacts between brecciated rock units should be virtually impossible to find. However, this writer has observed that at Howell, formation masses and even contacts are often traceable across the structure …
>
> This feature of the Howell structure is especially evident in the rocks of the Richmond Group, which were once considered post-deformation as they appear to have been deposited upon the structure proper. Even though this writer has demonstrated that the structure originated long after the Ordovician Richmond was deposited, the integrity of the mapped units in a distinct area still holds true. The same formational mass "integrity" may be generally true for the older Ordivician rock units. This has been locally observed but not fully investigated …
>
> The major problem in this assertion is the absence of a widespread zone of mixed Richmond and Nashville rocks to match the lithologic zones in brecciated older Ordovician units …
>
> Only in scattered localities have Fernvale fragments been found in lower "Nashville" breccias …
>
> One other zone that may be classified as a mixed zone is the rock in the area of high ground which as mentioned before, appears to have chert and sand mixed with certain sulfides, clays and carbonaceous material.
>
> This may be a mixed zone of reworked lithologies present before deformation. These lithologies might include Silurian (Brassfield), and Devonian (Hardin sandstone or basal sand of Chattanooga Shale), all of which could have lain within a few feet of each other before deformation. This would, of course, entail an unconformity in that no Silurian and Devonian would have been present between the Brassfield and the Chattanooga. (Woodruff, 1968: 36,

Figure 14: A photograph which shows a possible breccia injection vein that crosses relict bedding (after Woodruff, 1968: 37).

Figure 15: A photograph of a "Breccia vein showing flow pattern of fine-grained brecciated particles around larger fragments." (after Woodruff, 1968: 38).

40–41).

Miller (1974: 25–26) also notes this unconformity in the geologic history of Tennessee:

> All of the Silurian rocks in Tennessee formed in marine or near shore environments …
>
> There was uplift of the land and some erosion at the end of Silurian time … but in most places it is not possible to determine how much, for two subsequent major episodes of erosion during the Devonian in some places removed all the rocks overlying the Middle Ordovician …
>
> There was renewed uplift after the deposition of the Pegram sediments, and this new episode of erosion was to result in one of the most important unconformities in Paleozoic rocks of this region. Much of the Devonian sediments, as well as extensive areas of Silurian and Ordovician rocks, were removed by erosion.
>
> When the Late Devonian sea advanced across the land, conditions had changed dramatically compared with other invasions of the ocean, and the environment was like few others in all of the geologic history of this region. The sea eventually spread over much of the east-central United States, depositing a black, carbonaceous mud over hundreds of thousands of square miles. This black mud, containing rotted organic matter, became the Chattanooga Shale.

Woodruff (1968: 41) again notes an unusual feature of the Howell Structure:

> It has been noticed in studying the Howell structure that the courser-grained rock units are more apt to be brecciated whereas the finer-grained rocks are less likely to be so deformed …

Woodruff (ibid.) noticed this phenomenon in the "… dove-like cryptocrystalline limestones …" which were not often brecciated. Occasionally Woodruff came across fragments of the 'dove' mixed with a brecciated unit and at least at one location he decided that the 'dove' was itself the breccia matrix.

Figure 16: Photographs of 'plum-pudding breccias'; the right hand image is a close-up view that shows identical lithologies of fragments and matrix (after Woodruff, 1968: 39).

> However, the dove-like zones (beds) have remained intact. The dove, therefore, has maintained its own lithologic integrity … (ibid.).

The puzzling aspect was that these seemingly-undisturbed units were within the area of most intense deformation. Woodruff (1968: 41–42, 44) discusses the possible mechanisms through which this unexpected result could have occurred:

> This has led to speculation by some observers that the structure may have been caused by diagenetic processes such as slumping of unconsolidated sediments, repeated time and time again during geologic time. By this speculation, there would be periods of deposition between the times during which the breccias were formed. The rocks deposited during these inter-breccia periods would be the undisturbed crypto-grained dove-like units … However, this sedimentary hypothesis cannot explain the extreme localization of deformation within a circular area and the presence of some radiating joint patterns as seen and measured in outcrops in creek beds bordering the structure.

Figure 17: A photograph of a breccia sill (after Woodruff, 1968: 43).

> Localized solution activity is also unsatisfactory in that it would seem to call for uplift, before the process of solution could work in such a limited area. No such uplift is observed.
>
> The explanation of that phenomenon may be better dealt with in terms of the more explosive processes, which are believed to have taken place here. One such explanation would be that the undisturbed bed [lying] flat upon [the] breccia is another example of breccia injection. Under great pressures breccia might behave as a slurry and may cross lithologic features. It has been mentioned that "breccia injection veins" have been observed; this then would be an example of a "breccia sill …"
>
> Another hypothesis concerning such a phenomenon would be the inconsistent behavior of shock waves in rocks of different lithologic types. Generally, the cryptograined rocks are not brecciated, although subjected to forces capable of granulating coarser rocks. Therefore, this writer postulates that there is a definite relationship between rock textures and shock transmission. Thus, the fine-grained dove-like limestones transmit the shock waves, but at the same time are not affected by the shock in a noticeable way. The coarser-grained units then receive the trans-mitted wave and amplify it from one grain boundary to the next, causing fragmentation. (The parallel that this writer draws is the behavior of earthquake waves in areas of sound bedrock as opposed to earthquake behavior in loose alluvial fill. The bedrock areas act as a unit in transmitting the wave, while the loosely consolidated material amplifies the "shock," causing the greatest destruction). The coarser-grained rocks do not behave as a distinct unit; the dove-like members do.

Figure 17 is a photograph taken by Woodruff (1968: 43) showing a breccia sill he investigated at the Howell Structure.

In the most recently-published investigation of the Howell Structure breccias, Milam et al. (2015) report on the analysis of limestone breccia samples obtained from Howell surface exposures and provided by R.G. Stearns, Professor Emeritus from Vanderbilt University (Nashville). X-ray diffraction (XRD) spectral analyses of breccias from the Howell Structure were compared with unshocked, optically clear calcite in an effort to identify diffraction peak broadening that can occur in the XRD spectra of shocked carbonates. Initial results for three of seven samples were consistent with shocked calcite. Full width half maximum values for these three samples were consistent with peak broadening observed in limestone from confirmed terrestrial impact sites, including Sierra Madera and Steinheim. However, this magnitude of peak broadening is also observed in some tectonically-deformed non-impact limestones. Milam et al. (ibid.) note that there is no evidence of tectonism in the immediate vicinity of Howell, so shock metamorphism of carbonate breccias due to impact is indicated and an impact origin for the Howell Structure is favored.

7 SHATTER CONES, SHOCKED QUARTZ, AND DRILL CORES

Dietz (1960: 1781) states that

> Volcanic explosions are steam explosions involving pressures of not more than several hundred atmospheres, so it is extremely doubtful that a shock wave can be developed in rock as a part of volcanic phenomena.

He points out that a meteorite impact is capable of generating a shock wave:

> A giant meteorite (that is, one which is not appreciably decelerated by passage through the atmosphere) should on average strike the earth with a velocity of about 15,000 meters per second. A principal effect of this impact is the generation of an intense and high-velocity shock wave which spreads out from the impact point, or "ground zero," and engulfs a great volume of rock before it finally decays into an

elastic wave. (ibid.).

French (1998: 36) states that

> Shatter cones are the only distinctive and unique shock-deformation feature that develops on a megascopic (hand specimen to outcrop) scale.

Dietz (1960: 1782) searched the Howell site for shatter cones as proof of impact, but he found that "Rock outcrops at the Howell structure are too poorly developed to permit any intensive search there …" (ibid.). Miller (1974: 56), however, notes that "Some features that may be shatter cones have been found, but they are indistinct."

Shatter cones have been used as indicators of meteoric impact, and are typically oriented so that the tips of the cones point toward the shock, or 'ground zero', of the meteorite impact. Therefore, "… shattercones are useful in determining … whether the explosion originated from above or below." (Woodruff, 1968: 23). He continues:

> Shattercones have not been previously identified in the Howell area, but this writer has found one location in which crudely formed cones may be present … (ibid.).

Figure 18 shows what Woodruff (1968: 24) calls possible shatter cones. The photographic equipment he used during the 1960s did not produce the clear images he desired, so Figure 19 shows this same photograph with a Mylar film overlay marked to show the features he saw that did not show up as well as he desired on the grainy photograph. Likewise, Figure 20 shows a "Poorly formed shattercone …" and Figure 21 shows the same photograph, again with the features he saw in person indicated by the overlay (Woodruff: 1968: 25). The fact that Woodruff considered this later example to be a poor example of a shatter cone does not preclude an impact origin.

Woodruff searched the Howell site for other evidence of shock, and noticed that the texture and mineralogy of specimens he found on the higher ground located in the northeastern section of the Howell Structure were "… so unlike anything else seen in the Howell area, that thin sections were made for further study …" (Woodruff, 1968: 59). This area is a mixed zone consisting of sand and chert, sulfides and carbonaceous material, and the outcrops here may be fossil rim material or "… a basal lens of the basal sand of the Chattanooga Shale …" which would have been deposited "… in a marsh or in deep stagnant water …" (ibid.). The thin sections studied in this petrographic investigation were found to be "… predominately quartz or other silica material, such as chert …" (Woodruff, 1968: 61).

Figure 18: A photograph of possible shatter cones (after Woodruff, 1968: 24).

Figure 19: Use of an overlay to indicate the features that may be shatter cones (after Woodruff, 1968: 24).

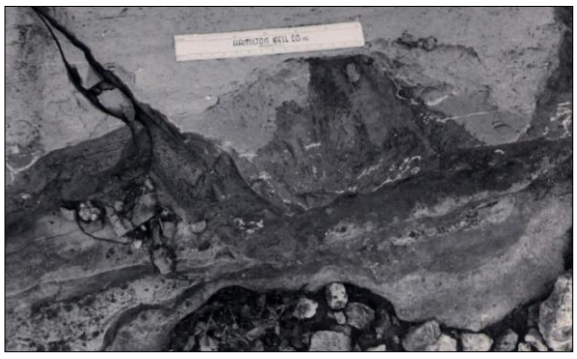

Figure 20: A photograph of a poorly-formed shatter cone (after Woodruff, 1968: 25).

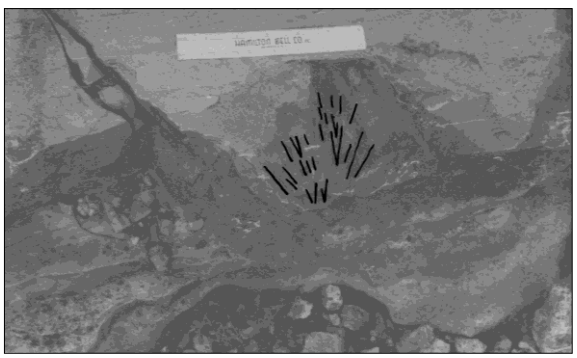

Figure 21: Use of an overlay to indicate the poorly-formed shatter cone (after Woodruff, 1968: 25).

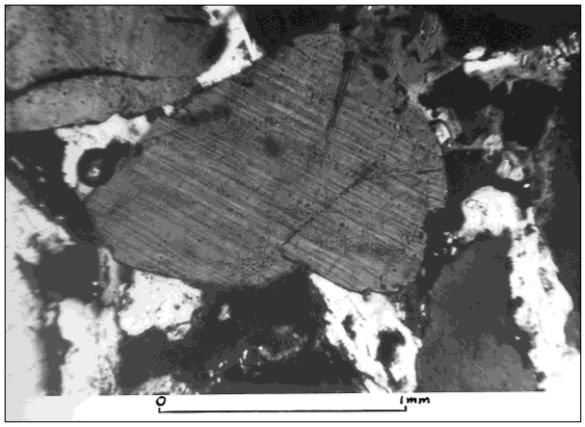

Figure 22: A thin section showing a quartz grain with planar features (after Woodruff: 1968: 62).

This investigation found in some quartz grains "… a definite lineation … or sometimes sets of lineation … so prominent so as to indicate one or two directions of cleavage …" (ibid.). Wilson and Stearns (1968: 153) point out that their investigation of the Wells Creek confirmed impact structure determined that "The most severe deformation noted in quartz is somewhat widely spaced fracturing." Figure 22 shows a thin section of a quartz grain photographed in polarized light displaying planar features (after Woodruff, 1968: 60). Another quartz grain displayed 'patchy extinction', indicating that it was subjected to sufficient stress to granulate and then re-indurate so as to retain its original form as a single grain. Woodruff (1968: 61) also found several samples in which

> Other possible indications of shock are seen where certain quartz grains, or what appear to be quartz grains, are partially or entirely isotropized … [and] In certain areas of the thin sections which macroscopically appear to be stringers of glauconite and possibly hematite, it is seen in thin section to consist of something resembling flow of finely divided quartz. The lineation of the glauconite and the flow-like trend of the smaller silicious material aligns with each other. (ibid.).

Woodruff states that some quartz grains were found to be

> … completely fragmented in certain areas of the thin sections … usually where the section is thinner than usual, as around the edge of the section …

and he believes that "This fragmentation may represent incipient fractures due to stress …" (ibid.). Figure 23 shows two samples found by Woodruff at the Howell site. One thin section, photographed in plain light, he calls a micro-breccia, and he states that it is a single quartz grain which displays a "… mosaic of fractures in thin section …" (Woodruff, 1968: 62). The second thin section, photographed in polarized light, shows the "… flow of finely divided particles …" (ibid.). Woodruff (1968: 63) then makes the following observation from his petrographic study:

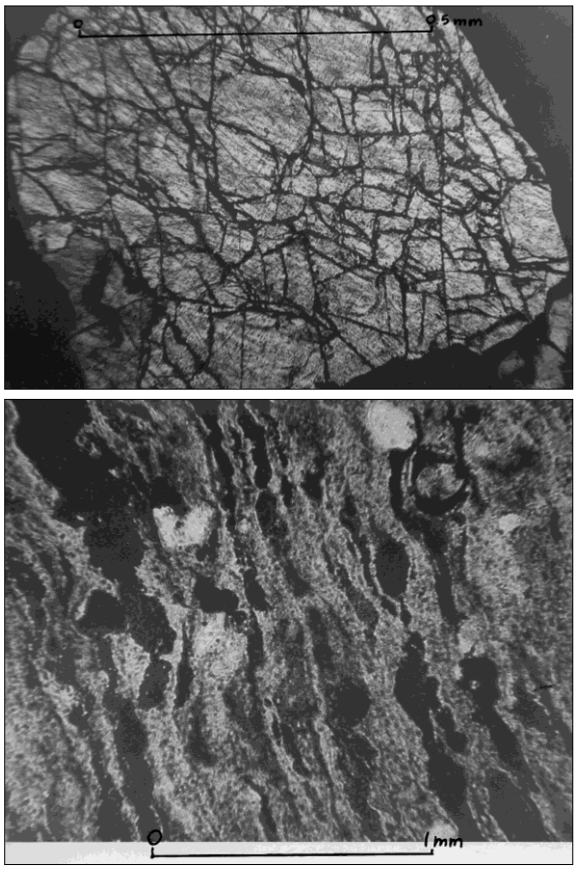

Figure 23: Thin sections showing two quartz grain samples displaying (top) a 'micro-breccia', and (bottom) "… the flow of finely divided particles ..." (after Woodruff: 1968: 63).

> The rocks have constituent materials that have been subjected to severe stress, but at the same time, may contain material that has not been so subjected. There, it seems most likely that the material in consideration has been reworked, possibly even reworked rim material.

Woodruff (1968: 65) believes that the results of this petrographic study indicate that shock metamorphism has taken place, but unfortunately "… these thin sections did not survive the passage of 35 years of time and are lost for further study …" (Deane et al., 2004: 2). More samples from Howell were therefore required for a detailed investigation using modern technology.

In 2003, Deane and Milam were members of a team that made two trips to the Howell Structure in order "… to search for evidence of shock metamorphism in local lithologies …" (Deane et al., 2004: 2). The team gathered samples of limestone breccias from creek beds in the central part of the disturbed area, as well as samples of the Leipers and Catheys Formation (a fine-grained, thin to medium-bedded Ordovician limestone exposed at the base of the hills on the eastern side of the site), but could not obtain a micro-brecciated sample similar to the one reported and photographed by Woodruff. But they did find and analyze the 'powdered limestone'

breccia reported by Born and Wilson (ibid.). They stated that

> Thin sections were produced for all samples. All observed quartz grains displayed substantial micro-fragmentation. However, no unequivocal evidence of shock metamorphism such as melt, flow, or planar deformation features (PDFs) was found … (ibid.).

Woodruff (1968: 19) points out that in many structures such as Howell, geological processes have removed many of the characteristic features that are considered unequivocal indicators of shock due to impact, including coesite and stishovite, or isotropized quartz. Wilson and Stearns (1968: 152) noted that during their spectrographic study of breccias located within Wells Creek, a confirmed impact structure, no coesite or stishovite was found either, and that

> Although these dense materials were not found, their absence is not considered to preclude an impact origin of the structure …" (ibid.).

Woodruff (1968: 19) notes that "Meteorite fragments would be conclusive evidence, but, unhappily, this is the rarest evidence." Howell is far too old for such fragments to have survived the passage of time. Woodruff (1968: 20), therefore, discusses alternate means of determining whether a structure is the result of a meteorite impact:

> Ultimately, one of the few certain means of determining whether a structure is formed by meteoric or terrestrial process is by subsurface study. If the area of deformation has a lower limit above the (igneous-metamorphic) basement complex it is then concluded to be of meteoric origin. However, this is contingent upon the size of the deformed area. Meteor impact may well yield deformation to such depths as to involve basement and be impractical to drill through.

Woodruff (1968: 65) points out that

> The information gained by NASA's drilling (John Bensko, personal communication) is that the structure has a bottom in stratigraphic sequence and is thus lens-shaped at depth instead of being a breccia pipe.

Since the drill holes at Howell went through breccias and then penetrated into undisturbed rock, an impact origin was suggested, and this was recently confirmed when Bensko made cores available to Milam et al. (2015), and their analyses revealed clear evidence of shock metamorphism.

8 CONCLUDING REMARKS

Woodruff's 'shatter cones' are suggestive at best and no evidence of shocked quartz has been found at the Howell site, but we believe that the clear evidence of shock metamorphism recently assembled by Milam et al. (2015) suggests that the Howell Structure is indeed an old impact site—even though perhaps 80–90% of the crater has been removed by erosion. However, the first author of this paper feels that the evidence for an impact origin, although strong, is still not conclusive, and that for the moment the Howell Structure must remain one of Tennessee's two suspected meteorite impact sites.

Yet not everyone agrees with this conclusion. Based on his own investigations, Woodruff (1968: 29) concluded that the Howell Structure is "… the ancient eroded equivalent of a meteor impact crater …", and he cites the following evidence in support of this origin:

> The criteria used in this conclusion are based on the morphology of the structure, subsurface information, and petrography. The roughly circular-elliptical appearance, and radiating joint patterns are morphological indicators of such an origin, as are breccias, *but neither of these are [sic] conclusive*. (Woodruff, 1968: 65; our italics).

Miller (1974: 56) also concluded that "Overall, the evidence indicates the Howell Structure was formed by meteorite impact."

With so much of the original structure removed by erosion, it may be that proof of meteoric impact will never be forthcoming, but we hope that sites like the Howell Structure will encourage research into impact signatures in limestone that are associated with metamorphism at low shock pressures.

9 ACKNOWLEDGMENTS

The first author wishes to thank Marvin Berwind for sharing his time and expertise during a field trip to the Howell Structure. We also would like to thank Professors Martin Beech (University of Regina, Canada), Christian Koeberl (University of Vienna, Austria) and Wolf Reimold (Museum für Naturkunde and the Humboldt-Universität, Berlin, Germany) for comments that were helpful in allowing us to complete this paper.

10 REFERENCES

Baldwin, R.B., 1949. *The Face of the Moon.* Chicago, University of Chicago Press.

Baldwin, R.B., 1963. *The Measure of the Moon.* Chicago, University of Chicago Press.

Baratoux, D., and Melosh, H.J., 2003. The formation of shatter cones by shockwave interference during impacting. *Earth and Planetary Science Letters*, 216, 43–54.

Berwind, M., 2006. Field Trip to the Wells Creek Basin Cryptoexplosive Structure, Stewart and Houston Counties, Tennessee. Tennessee Division of Geology.

Berwind, M., 2007. Meteorite impact structures in Tennessee. *The Tennessee Conservationist*, 73(3), 15–18.

Boon, J.D., and Albritton, C.C., 1937. Meteorite scars in ancient rocks. *Field and Laboratory*, 5(2), 53–64.

Born, K.E., and Wilson, C.W., 1939. The Howell Structure, Lincoln County, Tennessee. *Journal of Geology*, 47, 371–388.

Bucher, W.H., 1936. Cryptovolcanic structures in the United States. *16th International Geological Congress*, 2, 1055–1083.

Collins, G.S., Melosh, H.J., and Ivanov, B.A., 2004. Modeling damage and deformation in impact simulations. *Meteoritics and Planetary Science*, 39, 217–231.

Collins, G.S., Melosh, H.J., and Marcus, R.A., 2005. Earth Impact Effects program: a web-based computer program for calculating the regional environmental consequences of a meteoroid impact on Earth. *Meteoritics and Planetary Science*, 40, 817–840.

Croft, S.K., 1977. Energies of formation for ejecta blankets of giant impacts. In Roddy, Pepin and Merrill, 1279–1296.

de Vet, S.J., and de Bruyn, J.R., 2007. Shape of impact craters in granular media. *Physical Review E*, 76, 4, 041306.

Deane, B., Lee, P., Milam, K.A., Evenick, J.C., and Zawislak, R.L., 2004. The Howell Structure, Lincoln County, Tennessee: a review of past and current research. *Lunar and Planetary Science*, XXXV, 1692.

Deane, B., Milam, K.A., Stockstill, K.R., and Lee, P.C., 2006. The Dycus Disturbance, a second impact crater in Jackson County, Tennessee? *Lunar and Planetary Science*, XXXVII, 1358.

Dietz, R.S., 1960. Meteorite impact suggested by shatter cones in rock. *Science*. 131, 1781–1784.

Evenick, J.C., Lee, P., and Deane, B., 2004. Flynn Creek impact structure: new insights from breccias, melt features, shatter cones, and remote sensing. *Lunar and Planetary Science*, XXXV, 1131.

Evenick, J.C., 2006. Field Guide to the Flynn Creek Impact Structure. University of Tennessee, Knoxville, Tennessee.

Ferriére, L., Lubala, F.R.T., Osinski, G.R., and Kaseti, P.K., 2011. The newly confirmed Luizi Impact Structure, Democratic Republic of Congo – insights into central uplift formation and post-impact erosion. *Geology*, 39, 851–854.

Ford, J., Orchiston, W., and Clendening, R., 2012. The Wells Creek meteorite impact site and changing views on impact cratering. *Journal of Astronomical History and Heritage*, 15, 159–178.

Ford, J., Orchiston, W., and Clendening, R., 2013. The Flynn Creek meteorite impact site and changing views on impact cratering. *Journal of Astronomical History and Heritage*, 16, 127–183.

Ford, J.R.H., Orchiston, W., and Clendening, R., 2014. An historical perspective on the suspected meteorite impact sites of Tennessee.1: The Dycus Structure. *Journal of Astronomical History and Heritage*, 17, 352–364.

French, B.M., and Short, N.M. (eds.), 1968. *Shock Metamorphism of Natural Materials*. Baltimore, Mono Book Corporation.

French, B.M., 1998. *Traces of Catastrophe, a Handbook of Shock-Metamorphic Effects in Terrestrial Meteorite Impact Structures.* Houston, Lunar and Planetary Institute.

French, B.M., Cordua, W.S., and Plescia, J.B., 2004. The Rock Elm Meteorite Impact Structure, Wisconsin: geology and shock-metamorphic effects in quartz. *Geological Society of America Bulletin*, 116, 200–218.

French, B.M., and Koeberl, C., 2010. The convincing identification of terrestrial meteorite impact structures; what works, what doesn't, and why. *Earth-Science Reviews*, 98, 123–170.

Gault, D.E., Quaide, W.L., and Oberbeck, V.R., 1968. Impact cratering mechanics and structures. In French and Short, 87–99.

Grieve, R.A.F., and Pilkington, M., 1996. The signature of terrestrial impacts. *AGSO Journal of Australian Geology and Geophysics*, 16, 399–420.

Housen, K.R., and Holsapple, K.A., 2011. Ejecta from impact craters. *Icarus,* 211, 856–875.

Hoyt, W.G., 1987. *Coon Mountain Controversies, Meteor Crater and the Development of Impact Theory.* Tucson, University of Arizona Press.

Ivanov, B.A., 1991. Impact crater processes. *Advances in Space Research*, 11, 67–75.

Kadono, T., 1999. Hypervelocity impact into low density material and cometary outburst. *Planetary and Space Science*, 47, 305–318.

Kadono, T., and Fujiwara, A., 2005. Cavity and crater depth in hypervelocity impact. *International Journal of Impact Engineering*, 31, 1309–1317.

Masaitis, V.L., 2005. Morphological, structural and lithological records of terrestrial impacts: an overview. *Australian Journal of Earth Sciences*, 52, 509–528.

Melosh, H.J., 1989. *Impact Cratering: A Geologic Process.* New York, Oxford University Press.

Milam, K.A. and Deane, B., 2005. Petrogenesis of central uplifts in complex terrestrial impact craters. *Lunar and Planetary Science*, XXXVI, 2161.

Milam, K.A., Deane, B., King, P.L., Lee, P.C., Hawkins, M., 2006. From the inside of a central uplift: The view from Hawkins Impact Cave. *Lunar and Planetary Science*, XXXVII**,** 1211.

Milam, K.A., Henderson, T., Deane, B., and Bensko, J., 2015. Petrography and XRD analysis of the Howell Structure, Lincoln County. *46th Lunar and Planetary Science Conference*, 2455.pdf.

Miller, R.A., 1974. *Geologic History of Tennessee*. State of Tennessee, Department of Environment and Conservation, Division of Geology*,* 74.

Mitchum, R.M., 1951. The Dycus Disturbance, Jackson County, Tennessee. M.Sc. Thesis, Vanderbilt University.

Nemchinov, I.V., Popova, O.P., and Teterev, A.V., 1999. Penetration of large meteoroids into the atmosphere: theory and observations*. Journal of Engineering Physics and Thermodynamics*, 72, 1194–1223.

Pierazzo, E., and Collins, G**.,** 2003. A brief introduction to hydrocode modeling of impact cratering. In Laeys, P., and Henning, D. (eds.). *Submarine Craters and Ejecta-Crater Correlation*. New York: Springer. Pp. 323–340.

Pilkington, M., and Grieve, R.A.F., 1992. The geophysical signature of terrestrial impact craters. *Reviews of Geophysics,* 30, 161–181.

Popova, O., 2005. Meteoroid ablation models. *Earth*, *Moon*, *and Planets,* 95, 303–319.

Price, B., 1991. Tennessee's mystery craters. *Tennessee Conservationist.* Tennessee Division of Geology, September/October issue, 22–26.

Roddy, D.J., 1968. The Flynn Creek Crater, Tennessee. In French and Short, 291–322.

Roddy, D.J., 1977a. Large-scale impact and explosion craters: comparisons of morphological and structural analogs. In Roddy, Pepin, and Merrill, 185–246.

Roddy, D.J., 1977b. Pre-impact conditions and cratering processes at the Flynn Creek Crater, Tennessee. In Roddy, Pepin and Merrill, 277–308.

Roddy, D.J., and Davis, L.K., 1977. Shatter cones formed in large-scale experimental explosion craters. In Roddy, Pepin, and Merrill, 715–750.

Roddy, D.J., Pepin, R.O., and Merrill, R.B. (eds.), 1977. *Impact and Explosion Cratering: Planetary and Terrestrial Implications.* New York, Pergamon Press.

Schaber, G.G., 2005. The U.S. Geological Survey, Branch of Astrogeology–A Chronology of Activities from Conception through the End of Project Apollo (1960–1973). *U.S. Geological Survey Open-File Report 2005-1190.*

Schedl, A., Mundy, L., Carte, K., 2010. Application of a paloestress piezometer to Jeptha Knob, Versailles and Dycus Structures. Are they meteorite impacts? *GeologicaL Society of America Abstracts with Programs,* 42, 5, 172.

Schieber, J., and Over, D.J., 2005. Sedimentary fill of the Late Devonian Flynn Creek Crater: a hard target marine impact. In Over, D.J., Morrow, J.R., and Wignall, P.B., (eds.). *Understanding Late Devonian and Permian-Triassic Biotic and Climatic Events.* Elsevier. Pp. 51–70.

Shoemaker, E.M., 1983. Asteroid and comet bombardment of the Earth. *Annual Reviews of Earth and Planetary Sciences*, 11, 461–494.

Stearns, R.G., Wilson, C.W., Tiedemann, H.A., Wilcox, J.T., and Marsh, P.S., 1968. The Wells Creek structure, Tennessee. In French and Short, 323–338.

Stöffler, D., and Langenhorst, F., 1994. Shock metamorphism of quartz in nature and experiment: I. Basic observation and theory. *Meteoritics*, 29, 155–181.

Wilson, C.W., 1953. Wilcox Deposits in explosion craters, Stewart County, Tennessee, and their relations to origin and age of Wells Creek Basin Structure. *Bulletin of the Geological Society of America,* 64, 753–768.

Wilson, C.W. and Stearns, R.G., 1966. Circumferential faulting around Wells Creek Basin, Houston and Stewart Counties, Tennessee – a manuscript by J.M. Safford and W.T. Lander, circa 1895. *Journal of the Tennessee Academy of Science*, 41, 1, 37–48.

Wilson, C.W. and Stearns, R.G., 1968. *Geology of the Wells Creek Structure, Tennessee*. State of Tennessee, Department of Environment and Conservation, Division of Geology, 68.

Woodruff, C.M., 1968. The Limits of Deformation of the Howell Structure, Lincoln County, Tennessee. M.Sc. Thesis, Vanderbilt University.

Wünnemann, K, Collins, G.S., and Melosh, H.J., 2006. A strain-based porosity model for use in hydrocode simulations of impacts and implications for transient crater growth in porous targets. *Icarus*, 180, 514–527.

Jana Ruth Ford is an instructor of physics and astronomy at Middle Tennessee State University in the USA, and recently completed a history of astronomy Ph.D. on the confirmed and suspected meteorite impact craters of Tennessee through the University of Southern Queensland. She was supervised by Wayne Orchiston and Ron Clendening. Her primary interest is in the history of Solar System astronomy. She was previously an observatory assistant at Vanderbilt University's Dyer Observatory and an astronomy educator at the Sudekum Planetarium in Nashville.

Professor Wayne Orchiston works at the National Astronomical Research Institute of Thailand and is an Adjunct Professor of Astronomy at the University of Southern Queensland in Toowooma, Australia. Wayne is interested in the history of astronomy and in meteoritics, and he welcomed the chance to combine these two research areas by supervising Jana Ruth Ford's Ph.D. thesis.

Ron Clendening is a geologist working for the Tennessee Division of Geology, the Geologic Survey for the State of Tennessee, USA. For the past six years he has worked in producing geological maps for the Division of Geology. Though his primary academic interest is in quaternary geomorphology, his professional work has mainly concentrated on groundwater, environmental and karst geology of the central limestone region of Tennessee. In addition to working as a professional geologist, he also worked as a soil scientist, producing soil mapping products for private interests, as well as local and state government agencies. He is a career-long member of Geological Society of America.